RESERVOIR SIMULATIONS INTEGRATED WITH GEOMECHANICS FOR WEST SAK RESERVOIR

A

PROJECT

Presented to the Faculty

of the University of Alaska Fairbanks

in Partial Fulfillment of the Requirements

for the Degree of

MASTER OF SCIENCE

By

Nitesh Chauhan

Fairbanks, Alaska

July 2014

COMMITTEE MEMBERS:

Dr. Santanu Khataniar

Dr. Abhijit Dandekar

Dr. Shirish Patil

Abstract

Geomechanics is the study of the mechanical behavior of geologic formations. Geomechanics plays an important role in the life of a well. Without a proper understanding of the geomechanics of a reservoir, the projects associated with it may run into problems related to drilling, completion, and production.

Geomechanics is important for issues such as wellbore integrity, sand production, and recovery in heavy oil reservoirs. While studying geomechanics, proper weight is given to mechanical properties such as effective mean stress, volumetric strain, etc., and the changes that these properties cause in other properties such as porosity, permeability, and yield state. The importance of analyzing geomechanics increases for complex reservoirs or reservoirs with heavy oil.

This project is a case study of the West Sak reservoir in the North Slope of Alaska. Waterflooding has been implemented as enhanced oil recovery method in the reservoir. In this study, a reservoir model is built to understand the behavior and importance of geomechanics for the reservoir. First, a fluid model is built. After that, reservoir simulation is carried out by building two cases: one coupled with geomechanics and one without geomechanics. Coupling geomechanics to simulations led to the consideration of many important mechanical properties such as stress, strain, subsidence etc. Once the importance of considering geomechanical properties is established, different injection and production pressure ranges are used to understand how pressure ranges affect the geomechanical properties. The sensitivity analysis defines safer pressure ranges contingent on whether the formation is yielding or not. The yielding criterion is based on Mohr's Coulomb failure criteria. In the case of waterflooding, injection pressure should be maintained at 3800 psi or lower and production at 1600 psi or higher. And if injection rates are used as the operating parameter, it should be maintained below 1000 bbls/day. It is also observed that injection pressure dominates the geomechanics of the reservoir.

Table of Contents

List of Figures

List of Tables

Acknowledgements

I take this opportunity to extend my appreciation to my advisor, Dr. Santanu Khataniar, for his continuous guidance, motivation, and support throughout my project work. I am really grateful to have found a mentor like him, someone with so much experience and knowledge. Under his encouragement and supervision I was able to finish this work in a timely and effective manner.

I am thankful to my committee members Dr. Abhijit Y. Dandekar and Dr. Shirish Patil. They guided me at each step and with their immense knowledge and experience provided me with insightful details that helped me make this work a valuable one.

I am very grateful to Kiran Venepalli and Thanh Nguyen at CMG for providing me continuous help and availability whenever needed.

In the end I would like to thank my family and friends without whose support this work would not have been possible.

Chapter One

Introduction

1.1 Overview

According to British Petroleum's (BP) Energy Outlook 2035, global energy consumption is expected to rise by 41% from 2012 to 2035. The projected value for this demand is 17566 million tons oil equivalent (TOE). Oil and gas will comprise 8.5 billion TOE of this total value. It is also predicted that the energy production will increase to 4816 TOE for oil and 4647 TOE for gas. (BP, 2013)

British Petroleum's forecast assumes that there will be technological advances in the oil and gas industry, particularly in production from complex reservoirs. The latest advances in horizontal drilling, hydro-fracturing, shale oil, and tight gas have helped the industry to achieve higher production, but concrete solutions to many problems have yet to be found. Some answers to these problems lie in the study and analysis of geomechanics.

In 1980, one of the first horizontal wells was drilled (King, 1993), in hope of producing oil and gas from reservoirs where vertical well drilling was not economical. It was soon realized that horizontal wells help reduce the cost of field development, as fewer wells are needed if horizontal wells are used. Multi-laterals extend the advantages of horizontal wells by reaching different layers; hence, one well can cover a larger production area.

A lot of oil is found in sandstone reservoirs. In such reservoirs, various issues such as sand production, well failure, drop in production due to subsidence, etc., are likely to occur. Sand influx can cause a variety of problems such as a drop in the productivity of the reservoir, erosion to the completion, and surface facilities. Sometimes the sand production is so drastic that sand starts to accumulate at the bottom of the well, ceasing oil production.

Sandstone reservoirs are made up of sand grains cemented together. Oil and gas reside in the pore spaces created by these grains. When hydrocarbons are produced, they cause a shear force on the surface of the grains. If the shear force is greater than the bond strength between the grains, the bonds will break. As soon as the bonds are broken, the sand grains become loose and tend to flow with the hydrocarbons. Sometimes sand grains form a sand arch while flowing towards the wellbore. If these sand arches are stable, as shown in figure 1, there will not be any more sand production, but if the drawdown pressure is increased further, the sand arches will be unstable and sand production will continue (Hall and Harrisberger, 1970). Even if there is no sand production, other issues such as subsidence may arise. Subsidence occurs when overburden pressure exceeds pore pressure.

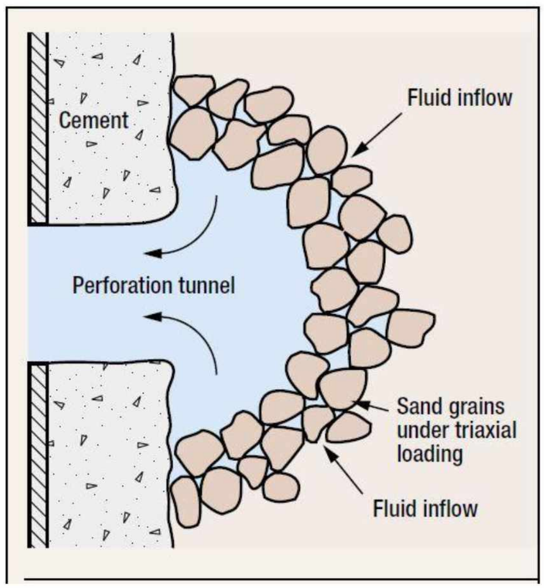

Figure 1: Geometry of a stable arch (Ott and Wood, 2001).

Well integrity is complicated, as it depends on various factors such as pressure drawdown, horizontal and vertical stresses, overburden stresses, quality of rock, and type of bonds, among others. Since reservoirs, well types and locations, perforations, and orientations vary widely; operating without considering geomechanics can be very dangerous.

1.2 Objective

The main focus of this study is to understand the role geomechanics plays in the life of a reservoir and how it can be used to understand various reservoir problems. To analyze the geomechanics in a reservoir in the North Slope, the following tasks are performed:

1. Build a fluid model for the selected reservoir.
2. Build a reservoir model and simulate production through the reservoir.
3. Couple geomechanics to the reservoir model.
4. Understand various geomechanical properties.
5. Based on the understanding of how geomechanical properties work, determine the operating parameters so that the chance of formation failure is minimized.

Chapter Two

Literature Review

2.1 Geomechanics

Geomechanics is derived from the Greek prefix geo- meaning earth and mechanics. Geomechanics is the branch of science which involves the study of soil, rock and the phenomenon associated with it. In the Petroleum industry, geomechanics is used to predict various factors, such as stresses, strains, young's modulus and Poisson's ratio. Various reservoir parameters such as bottomhole pressure, porosity and permeability are dependent upon the geomechanical factors.

Geomechanics depends upon various factors. The production of sand from any reservoir is dependent upon three main components:

1. Rock strength and other intrinsic geomechanical properties.
2. Regional stresses imposed on the perforation or wellbore.
3. Local loads imposed on the perforation or wellbore due to production, reduced pore pressures, and the presence of water. (Jonathan, 2009)

The above three are subdivided into the following five parts: Degree of consolidation, reduction in pore pressure throughout the life of a well, production rate, reservoir fluid viscosity, increasing water production throughout the life of a well (Ott and Wood, 2001).

2.1.1 Degree of Consolidation

Degree of consolidation is a property of rocks that describes the strength of the bonds between grains. Rocks that have stronger bonds are strongly consolidated and those that have weaker bonds are unconsolidated. Sometimes wells have strong intergranular bonds, but this bonding weakens with maturity or after a certain amount of production (Ott and Wood, 2001). Compressive strength is usually used to define the degree of consolidation of rocks. Poorly consolidated sandstone formations usually have a compressive strength that is less than 1,000 pounds per square inch (psi). The degree of consolidation can also be affected by various reservoir treatments such as acidization or steam flooding (Ott and Wood, 2001).

2.1.2 Reduction of Pore Pressure

With increase in depth, the pressure of the overlying layers on the underlying layers increases. This pressure is called overburden pressure. The reservoir pressure (pore pressure) balances this overburden. When production begins in a reservoir, this equilibrium is disturbed and leads to an overburden pressure higher than the reservoir pressure. Compaction of the reservoir rock due to a reduction in pore pressure can result in surface subsidence. For example, the Ekofisk central platform in the North Sea is reported to have sunk 10 feet in its first 10 years of existence due to subsidence. Sometimes, due to increase in this overburden pressure, the sand grains are crushed and start producing fines that start migrating with the oil and gas, leading to sand production (Ott and Wood, 2001).

2.1.3 Production Rate

The production from any reservoir is dependent on the pressure drawdown through a well. Pressure drawdown is the difference between reservoir pressure and bottomhole pressure. The velocity of the flow is determined based on the drawdown. When the fluid flows, it exerts a drag force on the sand grains in contact with it. If the drag force is greater than the compressive strength of the material, the material fails, leading to sand production.

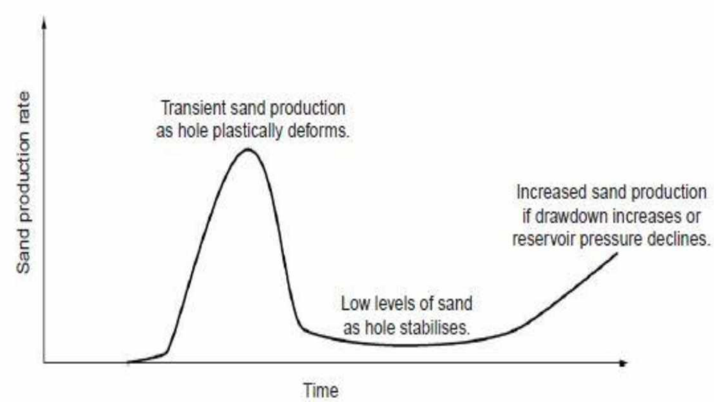

Figure 2: Typical sand production trend (Jonathan, 2009)

2.1.4 Reservoir Fluid Viscosity

The flow of reservoir fluid exerts frictional drag force on the formation's sand grains. This frictional drag force is directly related to the velocity and the viscosity of the reservoir fluid being produced. If the viscosity of the fluid is higher, it will exert a greater force on the formation.

2.1.5 Increasing Water Production

Sand production may begin, or increase, when water cut increases or water is produced through the oil formation. Cohesion is the bonding among different grains. The residual water saturation present in the reservoir provides some of this strength. If water fills the spaces between the grains, connate water starts to accumulate, leading to a decrease in cohesion strength (Muecke et al., 1979).

Water is capable of dissolving the cementation present in the reservoir. A higher water cut leads to a decrease in relative permeability to oil. As the relative permeability increases, so does the capillary pressure and the pressure required to produce oil. Once a higher pressure is applied across the formation, it leads to increased shear force and soil failure (Penberthy et al., 1992).

2.2 Role of Geomechanics

Geomechanics plays an important role in determining the effects of rock deformations caused by the pore pressure and temperature changes resulting from production and injection. Rock deformation affects porosity, permeability, and compressibility. The changes in pore pressure lead to a change in pore volume (Gutierrex et al., 1998).

Oil sands are particulate in nature. Their volumetric behavior changes based on loading conditions. When the grains are loaded they generally deform in an elastic manner but they can also override, shear, rotate, translate, or crush (Carlson, 2003; Li et al., 2003). The reservoirs can undergo two kinds of loading: isotropic or anisotropic. Under isotropic loading, the grains undergo very little reorientation relative to each other, while under anisotropic loading, the grains can undergo substantial reorientation.

Whenever reservoirs are produced they undergo both isotropic and shear stress loading (anisotropic). Generally, when enhanced oil recoveries are performed on the reservoirs, injection pressure results in an increase in pore pressure. This increase in pore pressure leads to a decrease in the effective stress and isotropic unloading. At a certain distance, an increase in the anisotropy would lead to shearing. This mechanism is exaggerated if the reservoir is poorly consolidated.

Once changes in shear stresses take place, they start influencing reservoir properties like porosity and permeability. These stress changes can also lead to subsidence issues. If the hardness of the sand grains is not high enough, there can be a considerable amount of crushing and a loss of grain properties such as porosity and permeability.

In the reservoir there can be two types of fluid flow and rock deformation coupling: stress permeability coupling and deformation fluid pressure coupling. In stress permeability coupling, changes in pore structure due to rock deformation affect permeability and fluid flow. In deformation fluid flow coupling, the rock deformation affects fluid pressure and vice versa (Guitierrex et al., 1998).

Reservoir deliverability is dependent on parameters such as fluid pressure, reservoir stresses, and fracture permeability during injection and production. Enhanced oil recovery methods such as miscible and immiscible gas injection, water flooding, and microbial injection may lead to near well contraction and a decrease in stress. In polymer injection, the stresses in the reservoir may increase due to high fluid viscosity and a decrease in formation permeability. Temperature variation may lead to rock expansion and contraction. Tensile failure happens when the tensile strength of the reservoir is less than the stresses. Shear failure occurs when the stresses are higher than the shear strength of the rock. All of these failure models are dominated by Mohr-Coulomb failure criteria. Once the rock fails, it starts to produce sand and causes losses (Teklu et al., 2012).

The Mohr-Coulomb theory is a model used to describe the response of materials to shear and normal stresses. Coulomb's friction is used to determine the combination of shear and normal stresses that will cause a fracture. Mohr circles can be used to know which principal stress can produce the combination of stresses and the angle of the fracture plane. Mohr-Coulomb failure criteria can be represented by plotting the shear strength of the material versus the applied normal stress. A linear envelope for the material failure will be obtained which can be shown by equation 1.

$$\tau = \sigma \tan(\Phi) + c \qquad (1)$$

where τ is shear strength, σ is normal stress, Φ is the slope of the failure envelope, and c is the intercept of the failure with the τ axis; c is also known as cohesion and Φ is called the angle of internal friction (Labuz, 2012).

2.2.1 Geomechanics for water production

According to Terzaghi's Principle (1943), the injection rate is directly related to the stress distribution near a wellbore or in the reservoir.

$$\sigma_{eff} = \sigma - \alpha p \qquad (2)$$

Where σ_{eff} is effective stress, σ is stress, α is Biot's coefficient, and p is pore pressure.

Biot's coefficient can be calculated using equation 3 (Mese and Tutuncu, 2000).

$$\alpha = 1 - \frac{K_b}{K_{grain}} \qquad (3)$$

Where K_b is the bulk modulus and K_{grain} is the grain modulus.

Murlaidharan et al. (2005) performed core experiments on fractured and unfractured sandstones. They stimulated stress conditions and measured fluid flow across the cores. They found that fluid flow in a fractured core is greater at a small confining stress. Fluid flow in a matrix may increase due to an increase in stresses. It is recommended to find the optimal stress conditions for recovery through lab experiments.

According to Fakcharoenphol et al. (2012), waterflood-induced stresses improve oil recovery in shale reservoirs. Kocabas (2004) developed a transient analytical model to study the temperature and stress distribution induced by non-isothermal fluid injection. He showed that in a porous medium with hard materials, cooling due to waterflooding can create tensile stresses which lead to new fractures or propagation of existing fractures.

Zekri et al. (2001) performed experiments to understand the effect of thermal shocks in carbonates. He found that cooling leads to a reduction in permeability for unfractured cores but it does not affect tight limestone. Cooling improves the permeability of fractured cores. Heating and cooling both reduce the fracture gradient.

2.2.2 Geomechanics for polymer EOR

The ultimate recovery depends on the injection rate. The stress changes due to increased pore pressure near injection wells or increased resistance factor and residual resistance factor can lead to changes in injection rate. (Teklu et al., 2012)

Khodaverdian et al. (2010) investigated the geomechanical effects of polymer flooding in an unconsolidated reservoir. In unconsolidated sands, polymer flooding can lead to shear failure. Shear failure can cause fault reactivation, fluid losses, and casing failure. Once these fractures are reactivated, they propagate in the direction of lower-permeability layers.

Zhou et al. (2010) used tri-axial tests to show that polymer flooding in an unconsolidated formation induces planar fractures. Shear dilation due to a decrease in stress lead to an increase in permeability and injectivity.

2.2.3 Geomechanics for thermal EOR

Thermo-elastic stress caused by temperature variation can alter the magnitude and direction of principal stress. Pore pressure change and sand production can change poro-elastic stresses. Poro-elastic stresses, in turn, change the effective principal stress (Teklu et al., 2012).

Bazagouta et al. (2009) performed core flooding experiments and SEM analysis of the Arab D sands. They found that an increase in effective stress and temperature causes a decrease in permeability.

Sanyal et al (1974) conducted experiments on unconsolidated sandstone to show that there can be a 60 - 80% decrease in permeability due to increase in temperature. Collins (2007) worked on the Steam Assisted Gravity Drainage (SAGD). He suggested that by increasing permeability and mobility makes higher production possible. If steam is injected at a higher rate, higher shear failure will lead to better production.

2.2.4 Geomechanics in CO_2 flooding

Gas flooding can lead to stress redistribution in reservoirs. It is generally caused by reservoir temperature cooling and pore pressure fluctuations. Other mechanisms, such as geochemical effects, can further change stresses (Teklu et al., 2012).

Alam et al. (2011) conducted CO_2 flooding experiments on cores of the Ekofisk and Tor sands of the North Sea. They measured petrophysical and mechanical properties of the cores before and after the CO_2 flooding. They found that permeability, porosity, and formation strength decrease after flooding.

Mohamed et al. (2011) performed experiments on limestone cores. They discussed the effects of supercritical CO_2 flooding on limestone reservoirs. Injection of $CaCl_2$ caused rock dissolution, whereas NaCl did not have any effect on the core. Patel et al (1987) studied CO_2 injection and water injection rates to show that CO_2 injection rate was lower than water injection rate for carbonate reservoirs.

Rui et al. (2009) showed that by increasing effective stress, displacement efficiency of the CO_2 flood can be increased in low-permeability fractured reservoirs. A higher effective stress can deform fractures more easily than pores, leading to a higher fractional reduction in fracture permeability than matrix permeability.

Chiaramonte et al. (2011) worked on the CO2 EOR and sequestration project in the Tensleep formation. They studied the effects of geomechanics and fractures on the reservoir. They concluded that due to reservoir integrity problems, CO_2 injection was not feasible there.

2.3 Completion techniques used in the Arctic environment

In 1995, ARCO Alaska began to evaluate multilateral technology and its application for adding more reserves in the Kuparuk basin (Bennion et al., 1998). In 2005, the first successful open hole horizontal completions were done in the Colville River field of the North Slope. Mohr-Coulomb's criteria is used to evaluate the sanding problems by Erwin. Further laboratory analysis is done to conclude that no sand control method is required (Erwin et al., 2005).

Wedman et al (1999) performed lab testing to show that fracturing with resin-coated proppant is an effective technique for sand control. They found conventional techniques of fracturing for sand control—then, gravel packing—not very effective. Single trip frac pack technique has also been applied in a few areas and continues to develop. The lab testing showed that epoxy-coated grains control sand very effectively. Lab tests included unconfined compressive strength tests, conductivity tests, and flow tests. For fracturing, tests for proppant sizing and perforation selection were done. The first field tests performed well for a year, then started producing sand or proppant. After modifying the completion procedures, 16 new wells were treated in Schrader Bluff, and no sand has been reported. Productivity indices of range 0.3 - 1 barrels/day/psi are reported.

Geehan et al. (1999) described the fracture geometry of the zones treated by fracturing for sand control. These zones are part of the Schrader Bluff (O sands) and West Sak (N sands) reservoirs.

For Schrader Bluff OA sand, when the drawdown was 1200 psi, no sand was produced. For N sand, at 1000 psi drawdown, sand is produced, and at 700 psi drawdown, no sand is produced.

In 2011, BP started a pilot project to test the applicability of cold heavy oil production with sand (CHOPS) in Alaskan reservoirs. The Ugnu reservoir was tested via a four-well-production pilot. Two horizontal wells with surface-drive progressive cavity pumps were selected for appraisal. 20% sand production was allowed to be sustained over the test period. 500 bopd oil production rates were reported from the two wells. Even though the project was technically viable, the pilot program stopped for economic reasons. (Young et al., 2010)

Burton et al (2005) described the sand management and exclusion techniques adopted in the North Slope. To understand the long-term implications of sand production, studies such as formation strength characterization, formation stress characterization, and failure analysis were done. Unconfined compressive strength (UCS) of 100 psi to 8000 psi is reported. Triaxial tests resulted in net vertical stress of 0.44 psi/ft and net horizontal minimum and maximum stress of 0.16 and 0.29 psi/ft. From modeling, it is concluded that rocks fail under all drawdown conditions at UCS of 550 psi and 810 psi for conventional wells with standard, non-oriented perforations. It is reported that wells have been allowed to produce with 1 to 2 barrels of sand per day per 1000 barrels of liquid per day without many operational problems in the West Sak reservoir. Sand management has been found to work at most places, and sand exclusion using slotted liners is also used in a few places. Because of the variability in the size of the produced sand, a unique sand control method cannot be defined.

In Canada, sand production is not considered a reservoir problem, but sand is produced with the fluids for better production rates. CHOPS is one of the most popular production techniques in Canadian fields. In fields such as the Clearwater formation in Cold Lake, Alberta, sand cuts of 40 to 50% during the first 10 months and a cumulative sand volume of 42000 ft^3 is reported (McCaffrey and Bowman, 1991). In the Celtic, Lindbergh, and Frog Lake fields in Alberta, sand production of 7000 ft^3 is associated with a cumulative gross fluid production of $3.2*10^5$ ft^3 (Loughead and Saltuklaroglu, 1992; Metwally and Solanki, 1995).

2.4 West Sak development

2.4.1 West Sak reservoir description

The West Sak field is located on the North Slope of Alaska. It is estimated to contain 7 - 15 billion barrels of heavy oil in place (Burton et al., 2005). The area covered by these reservoirs is around 300 square miles. These reservoirs lie at 3,000 to 4500 ft below sea level, and under 1800 feet of permafrost. As a result, the temperature of the reservoirs varies between 40° and 90° F. The viscosity of the oil present is very high due to the cold environment. The API gravity of the reservoir fluid ranges from 10.5 to 22.5 degrees. As these reservoirs are poorly consolidated, it is very tough to produce the heavy oil without producing some sand (AOGCC Pool statistics, 2004).

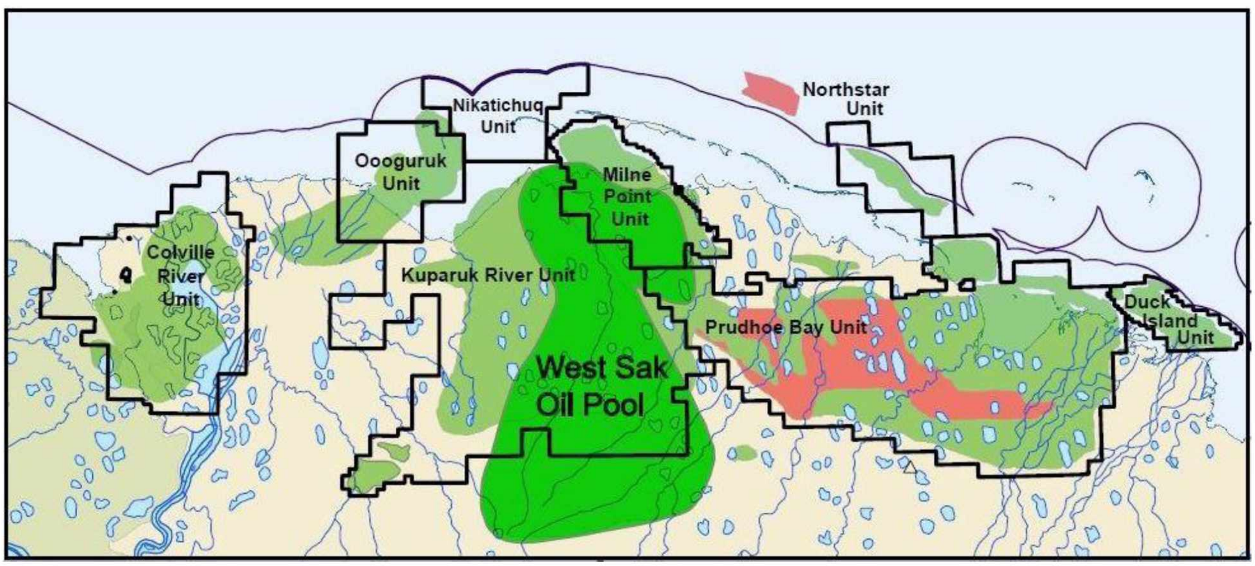

Figure 3: Map of West Sak reservoirs in ANS (AOGCC Pool statistics, 2004).

West Sak sands are an informally named member (subdivision) of the Late Cretaceous-aged Colville Group. The West Sak sands are roughly equivalent in age to the Schrader Bluff sands, which contain similar oil deposits, at Milne Point, Nikaitchuq, and in the Western Prudhoe Bay Unit (AOGCC Pool statistics, 2004). The West Sak sands are Late Cretaceous and early tertiary in age. They are deposited in a lower shore face to inner shelf setting by storm-generated waves and currents, and hence have good continuity (Burton et al., 2005). This shallow marine sand sequence is 400 feet thick (Werner, 1987).

The sands have a gentle dip of 1-2 degrees (130 feet per mile) from north to northeast. Grain size varies from very fine to fine-grained sands and silty sands. The predominant minerals in the sands are quartz, lithic fragments, and feldspar with traces of mica and glauconite (Panda et al., 1989). Sand beds are intersected by north-south trending faults. Faults and variations in stratigraphy have led to the entrapment of oil (Panda et al., 1989).

In 1971, ARCO discovered the West Sak sands under the Kuparuk fields. Two major sand groups have been reported, the upper West Sak Sand and the lower West Sak Sand. The upper West Sak sand is further subdivided into the D and B sands; the lower West Sak sand is also known as the A sand. The average thickness of the upper sand is 20 - 30 ft. A sands average 10 feet thick and are interbedded with sandstone and mudstone. The combined sand thickness is 80 - 90 ft. (Werner, 1987)

Three types of petrofacies can be identified based on porosity and permeability. Rock types 1 and 2 are the potential pay zones, while 3 is mainly mudstone. Porosity of rock type 1 varies from 25 to 35% and permeability varies from 200 to 1000 millidarcies. Oil saturation ranges from 40 to 75%, with a water saturation of 15 to 30%. For rock type 2, porosity varies from 20 to 30%, and a lower permeability range, from 15 - 200 millidarcies, is found. Oil saturation is also slightly lower as compared to type 1 (20 - 60%). A higher water saturation range, 25 -75%, is also reported (AOGCC Pool statistics, 2004).

2.4.2 West Sak reservoir development (Burton et al., 2005; Targac et al., 2005)

In 1970, exploration and appraisal wells were first drilled to delineate the extent of the West Sak reservoir. After a decade, 15 vertical wells in a 5-acre area were drilled to begin production. As the reservoir was not able to produce on its own, a 9 spot waterflood was chosen as the enhanced oil recovery method. In two years, 900,000 barrels of oil were produced from waterflooding.

In 1997, with new technologies and a better understanding of sand control techniques, new wells were drilled. This time, the well count per area was kept lower than before. Some wells were fracture stimulated. A rate of approximately 400 bopd is reported during this time period.

In 1999, 12 multilaterals were drilled in the reservoir, and in 2001, this value rose to 25. With the help of multilaterals, the wells were able to produce at a higher rate of 2000 bopd.

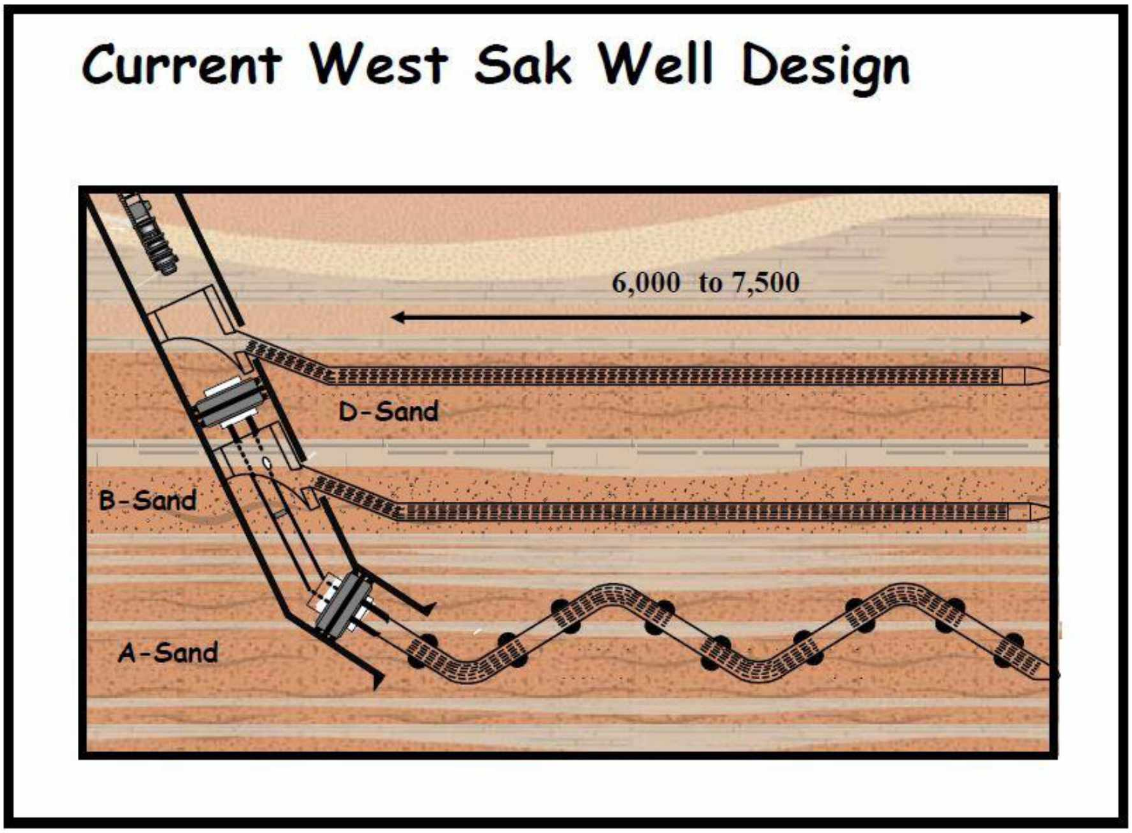

Figure 4: Generalized West Sak completion (Burton et al., 2005).

In 2003, the focus shifted to sand control techniques. Some of the wells were changed from screen completions to slotted liner completions.

2.5 Geomechanical model description (CMG - STARS Manual, 2014)

The plastic deformation model performs a finite-element elasto-plastic stress analysis of the reservoir formation using a specific set of displacement and traction boundary conditions. The theory of plasticity provides the theoretical description of the relationship between stresses and strains for a material which exhibits an elasto-plastic response.

During the elasto-plastic response, a material can behave elastically and plastically. When the material behaves elastically, its stress-strain properties can be described by any two material constants. Young's modulus and Poisson's ratio are examples of such constants. At a certain yield criterion, the material will start behaving plastically. Different materials have different elasto-plastic characteristics.

Plastic strain is considered to be irreversible after the material reaches a yield state at a certain stress level. The Mohr-Coulomb and Drucker-Prager, yield criteria describe the yield conditions of geologic materials. Once shear failure occurs, the nonlinear elastic models cannot predict the post-failure phenomena.

The behavior of cyclic loading and unloading as a result of cyclical injection and production processes can be modelled. During injection, the stress state at a location may reach a yield condition and begin to accumulate plastic strain.

The geomechanics module solves for the force equilibrium of the formation and calculates the volumetric dilatation/compression as a result of both elastic and plastic straining. The pore volume changes may be caused by a combination of compression/tension and shear stresses. These changes in pore volume and the associated changes in transmissibility are used in the reservoir model for calculating mass and energy balances in the reservoir.

Chapter Three:

Methodology and Model Construction

3.1 EOS model development

WinProp, an equation of state engineering tool from the CMG, is used to tune the EOS model and build a reservoir fluid model. Data such as fluid compositions and PVT tests including differential liberation, constant composition expansion, and saturation pressure are used. Most of the model data is from an extensive study of the West Sak fluid conducted by Sharma in 1990. Previous EOS models developed by Nourpour Aghbash (2013) and Morye (2007) are also studied. Nourpour Aghbash built the EOS model to understand the sequestration of CO_2 in the West Sak reservoir. Morye built the EOS model to perform compositional modeling. Nourpour Aghbash built a 10 component system with 3 pseudo-components, while Morye built a 9 component system with 1 pseudo-component.

Initial runs are carried out using the published composition of the West Sak (Sharma, 1990). The phase envelope and saturation pressure are simulated and compared with the experimental data. It is found that there is a large error in the saturation pressure values between the experimental and simulated data, which necessitates tuning. The initial composition used is shown in Table 1.

Table 1: Composition of West Sak fluid	
Component	Mol%
CO2	0.02
N2	0.03
C1	38.25
C2	0.86
C3	0.36
NC4	0.18
NC5	0.06
C6	0.2
C7	0.02
C8	0.01
C9	0.82
C10	1.5
C11	1.72
C12	1.35
C13	1.5
C14	1.8
C15	1.94
C16	1.8
C17	1.57
C18	1.8
C19	2.46
C21+ (MW = 455; SG = 0.875)	2.83

Peng Robinson's (1976) equation of state and gamma splitting function is used to split the C21+ fraction to C45+ fractions. Then, lumping is done to obtain one pseudo-component. As the computational time for any simulation study is dependent on the number of components present in the composition, the numbers of components is optimized to preserve fluid characteristics while decreasing run time.

The differential liberation test is simulated next, and results are compared to the experimental data. To find a suitable match between the experimental data and simulated values for critical pressure and temperature, acentric factors of the pseudo-components are regressed. During the regression, higher weights are given to saturation pressure, liquid density, and oil specific gravity. Higher weights are given based on the significance of the property. Once a good match for PVT properties is obtained, regression is done to match viscosity. Higher weights are given to oil and gas viscosities.

Table 2: **Differential liberation data (Sharma, 1990)**

P psia	Oil FVF bbl/stb	GOR scf/stb	Oil SG	Gas Z	Gas FVF	Gas SG	Oil viscosity cP	Gas viscosity cP
1704.7	1.070	207	0.9123	0.820	0.0070	0.570	45.2	0.0150
1514.7	1.062	187	0.9132	0.831	0.0083	0.571	50.2	0.0145
1314.7	1.055	165	0.9147	0.843	0.0098	0.579	51.8	0.0140
1114.7	1.047	144	0.9169	0.866	0.0118	0.567	59.3	0.0135
914.7	1.040	124	0.9191	0.887	0.0147	0.568	68.6	0.0130
714.7	1.033	96	0.9213	0.909	0.0194	0.568	83.4	0.0125
514.7	1.026	70	0.9250	0.933	0.0276	0.574	110.0	0.0120
314.7	1.019	42	0.9285	0.951	0.0456	0.573	150.0	0.0115
114.7	1.012	11	0.9334	0.985	0.1306	0.575	210.0	0.0110
14.7	1.008	0	0.9374	1.000	0.2000	0.661	272.7	0.0110

Table 3: Constant Composition expansion data (Sharma, 1990)		
P psia	**ROV**	**vol%**
7014.7	0.972	
6514.7	0.974	
6014.7	0.977	
5514.7	0.980	
5014.7	0.983	
4514.7	0.986	
4014.7	0.989	
3514.7	0.991	
3014.7	0.994	
2514.7	0.996	
2064.7	0.998	
1764.7	0.999	
1714.7	0.999	
1704.7	1.000	1.000
1447.7	1.032	0.974
1372.7	1.045	0.954
1258.7	1.067	0.934
1120.7	1.102	0.894
1021.7	1.134	0.878
907.7	1.180	0.844
818.7	1.227	0.798
705.7	1.305	0.762
594.7	1.415	0.685
460.2	1.622	0.605

Table 4: Weight distribution for EOS parameters	
Data point	Weight
Saturation pressure	50
GOR	100
Oil SG	100
Oil viscosity	100
Gas viscosity	100

Table 5 shows selected EOS parameter values before and after regression for pseudo-components. Table 6-8 shows the tuned EOS parameters and coefficients for the viscosity correlation.

Table 5: Changes in values of EOS Parameter			
Variable	Initial Value	Final Value	% Change
Pc	1.07E+01	1.25E+01	16.62
Tc	8.39E+02	1.01E+03	20
AF	9.62E-01	6.35E-01	-34

Table 6: Binary interaction coefficients									
	CO2	N2	CH4	C2H6	C3H8	NC4	NC5	FC6	C7+
CO2	0.00								
N2	0.000	0.000							
CH4	0.105	0.025	0.0000						
C2H6	0.130	0.010	0.0014	0.00000					
C3H8	0.125	0.090	0.0045	0.00088	0.00000				
NC4	0.115	0.095	0.0078	0.00259	0.00046	0.00000			
NC5	0.115	0.110	0.0109	0.00452	0.00143	0.00027	0.00000		
FC6	0.115	0.110	0.0134	0.00620	0.00243	0.00079	0.00013	0.0000	
C7+	0.138	0.117	0.0555	0.04026	0.02980	0.02314	0.01855	0.0156	0

Table 7: Viscosity correlation parameters				
Constant 1	Constant 2	Constant 3	Constant 4	Constant 5
1.02E-01	2.34E-02	5.85E-02	-4.08E-02	9.33E-03

Table 8: Changes in viscosity			
Variable	μ (viscosity), ft3/lb-mole		
	Initial Value	Final Value	% Change
C7+	1.7075E+00	1.7132E+00	0.34
CH4	6.3360E-02	5.0688E-02	-20

The good match between PVT properties and viscosity shows that the tuned EOS is capable of simulating the experimental values for all oil and gas properties. As the oil is heavy oil, at a pressure lower than 500 psia, viscosity values could not be matched.

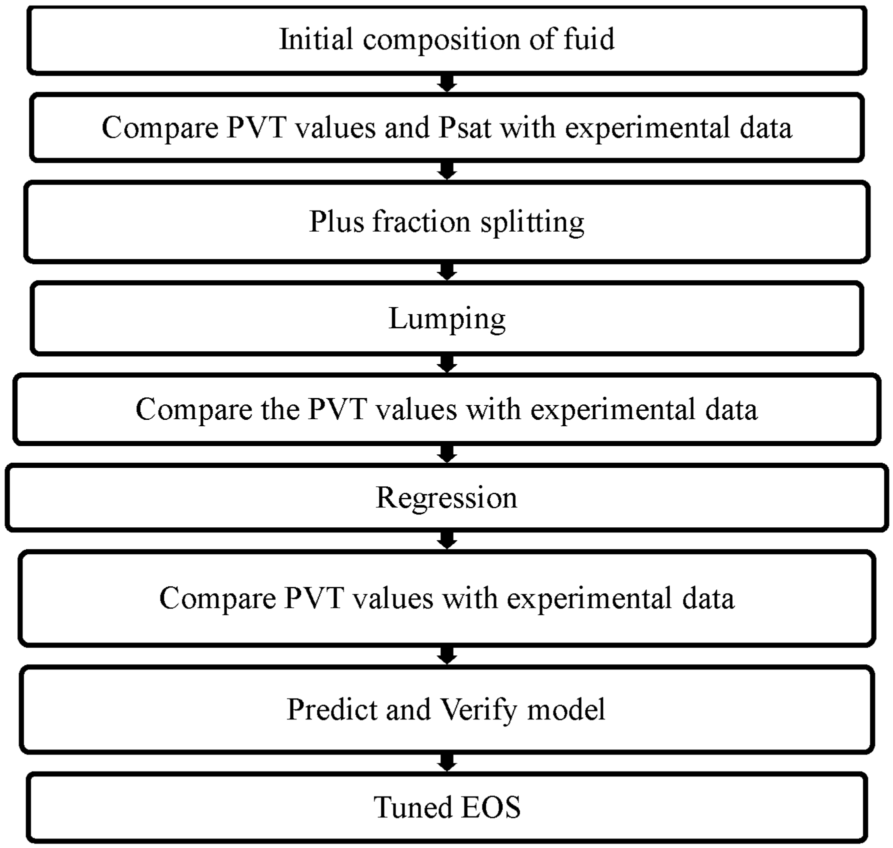

Figure 5: Tuning procedure for EOS.

3.2 Model development

After developing the EOS model, the next step was to study enhanced oil recovery in the West Sak reservoir, by building models and then coupling geomechanics to them to understand sand problems. A 40-acre area is chosen to run the simulation models. The reservoir is defined by five producing layers with shale layers in between. The layers have well defined porosity, permeability, and pay thickness values. The data to find the petrophysical properties of West Sak is obtained from the previously drilled wells.. The reservoir is divided into equal size grid blocks. There are 25 grid blocks in the I, J, and K directions. 9 layers are defined in the K direction. Hence, a total of 5625 grid blocks are simulated. As it is a comparative analysis, homogeneous representation of the reservoir should not hinder the sand control study. The reservoir properties are tabulated below, and a pictorial representation of the reservoir is shown in Figure 6.

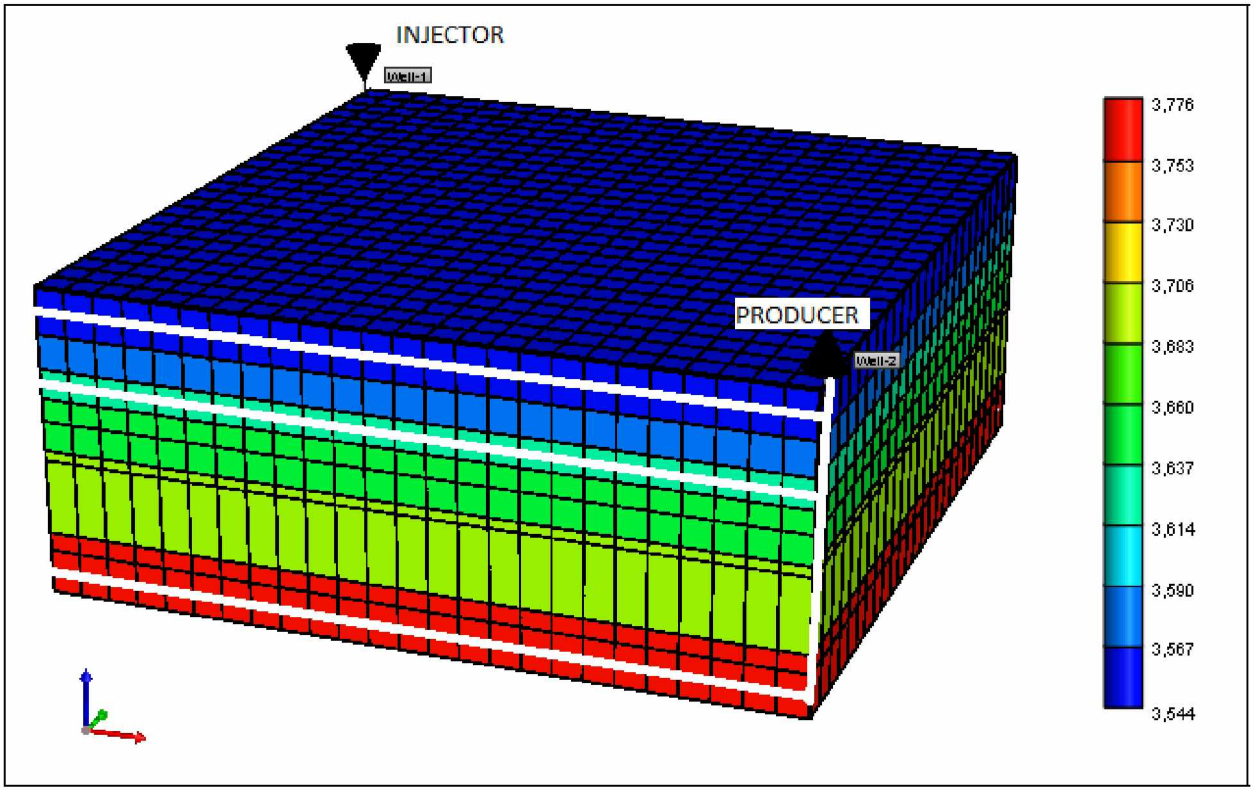

Figure 6: Layer top for the model

Table 9: West Sak reservoir properties (Bakshi et al., 1992)					
Layer No.	Sand	Interval, ft	Avg. porosity	Avg. water saturation	Net pay, ft
1	Upper 1	3544 - 3584	30%	24%	30
3	Upper 2	3614 - 3640	31%	31%	21
5	Upper 1	3660 - 3686	23%	45%	3
7	Lower 2	3695 - 3760	25%	47%	3
9	Lower 3	3776 - 3814	27%	41%	17

The relative permeability data is taken from a previous study done by Bakshi (1991).

3.2.1 Injection pressures

After building the model, simulation of enhanced oil recovery using water injection was carried out. Two wells were put in the model, both of them multilateral. One is specified as injector and the other as producer. The multilaterals are put in layers 1, 3, and 9. The layers are selected based on maximum potential for oil production.

The pressures used for the injector are 4200, 4000, 3800, 3500, 3000 and 2500 psi, while keeping the producer at 1600 psia. And for other case, water injection rates of 500 and 1000 barrels/day and producer at 1600 psia are used as the operating conditions. When sand scenarios are simulated, the producer is produced with a skin of +5. The skin is used to consider the near wellbore condition.

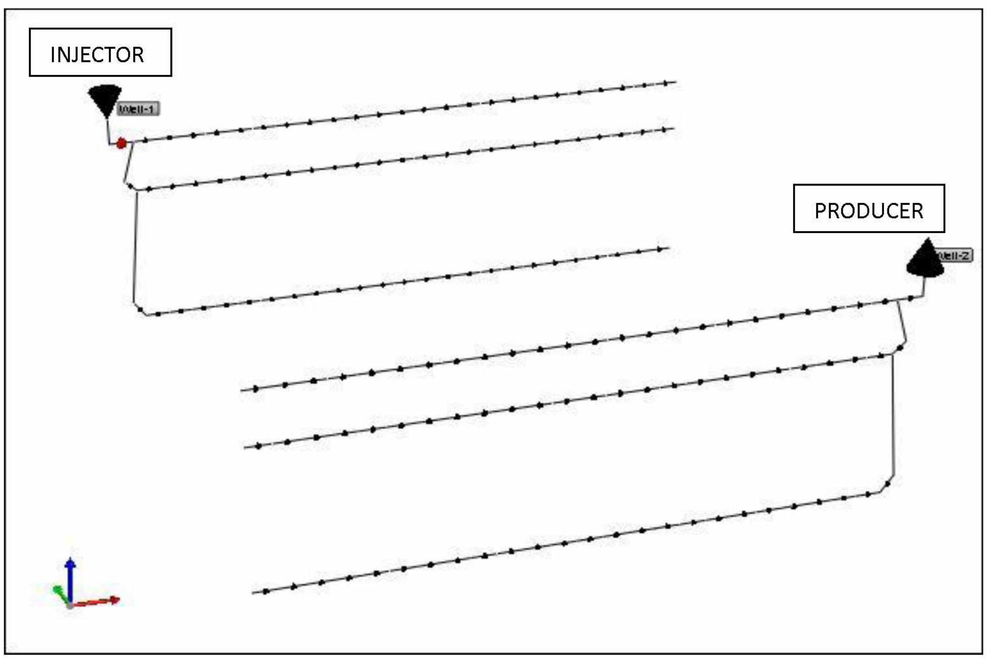

Figure 7: 3-D representation of the West Sak reservoir.

3.2.2 Geomechanics

For the reservoir, the Young's modulus is specified as 100,000 psi, cohesion pressure is defined at 100 psi, and Poisson's ratio is selected at 0.37. A low cohesion is selected to allow the formation to yield. As no data was found regarding the initial stresses, an initial stress of 2500 psi is set in the x, y and z directions. The reservoir is defined as an elasto-plastic material and governed by the Mohr's Coulomb criteria for failure (Hallam et al., 1991).

Chapter Four

Results

4.1 EOS tuning

The initial phase envelope of the un-tuned model is given below.

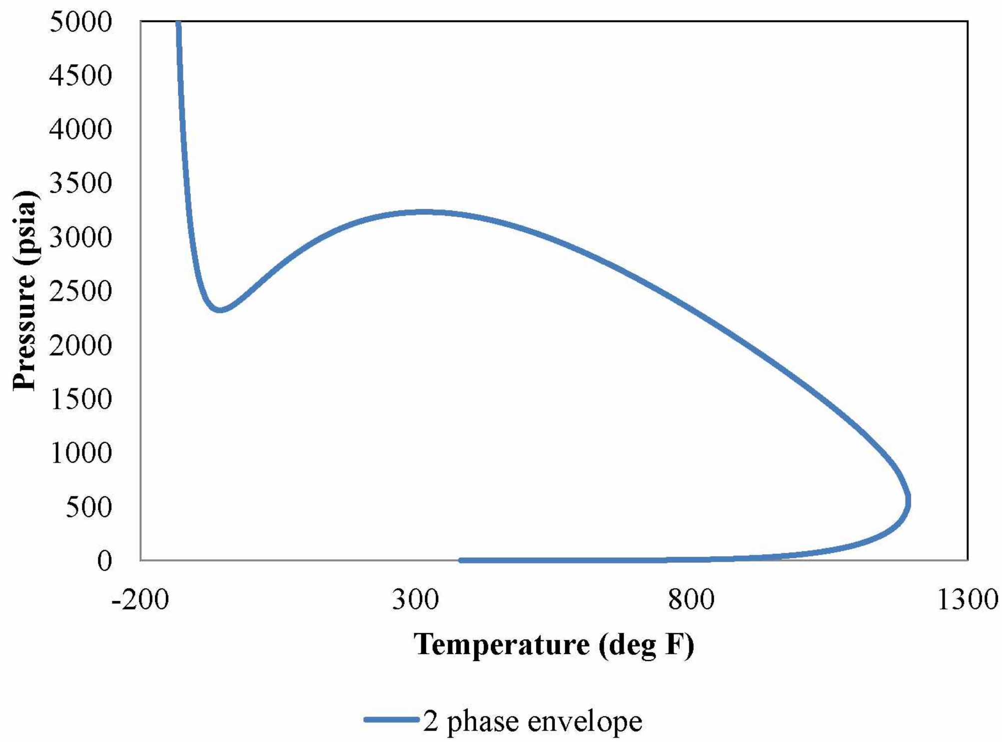

Figure 8: Phase envelope before tuning.

The saturation pressure value predicted by the un-tuned equation of state is 2834.015 psia at a temperature of 80^{o} F. The experimental value given in the literature is 1704 psia. The percentage error is 66.315 %. After tuning the model, the saturation pressure value obtained is 1706.84 psia, and the improvement can be seen through the PT envelope obtained.

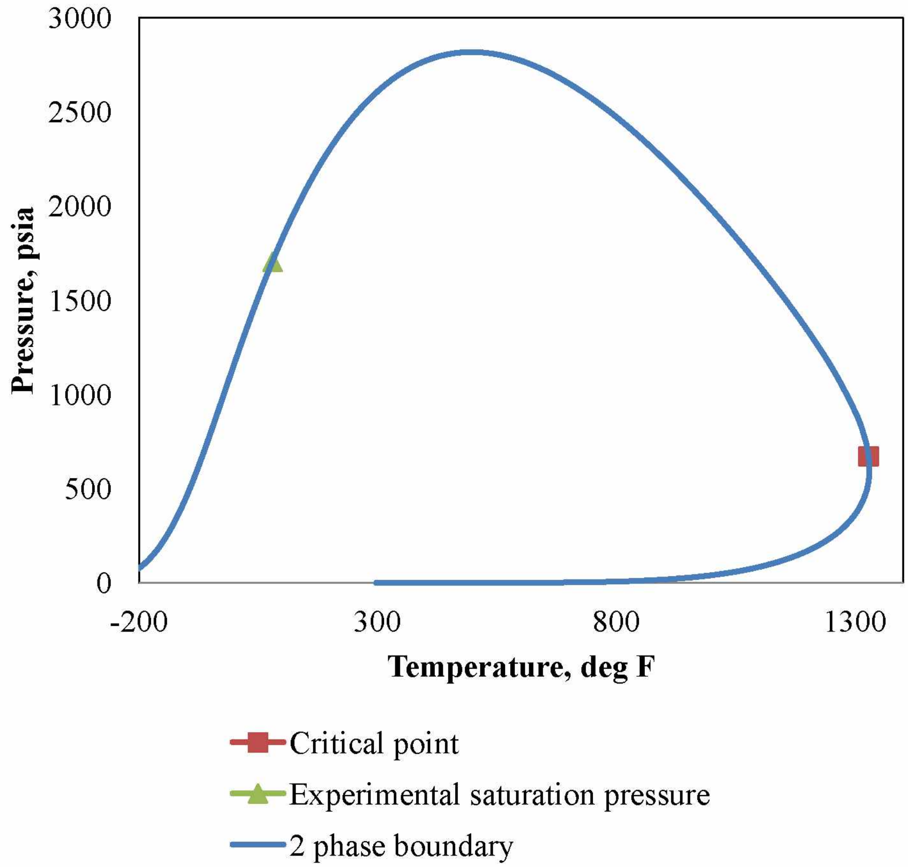

Figure 9: Phase envelope after tuning.

After the regression, the final composition and properties of the components are given below.

Table 10: West Sak reservoir fluid description

Comp.	Z, mole fraction	Pc, psia	Tc, R	Vc, l/mole	MW	Acentric factor	Para chor	Vol. shift
CO2	0.0001595	1069.79	547.56	0.094	44.01	0.225	78	0
N2	0.00031901	492.28	227.16	0.0895	28.013	0.04	41	0
CH4	0.38213901	667.15	343.08	0.099	16.043	0.008	77	0
C2H6	0.00854337	708.29	549.72	0.148	30.07	0.098	108	0
C3H8	0.00357885	615.72	665.64	0.203	44.097	0.152	150.3	0
NC4	0.00178444	551.06	765.36	0.255	58.124	0.193	189.9	0
NC5	0.00063801	489.34	845.28	0.304	72.151	0.251	231.5	0
FC6	0.00199379	476.99	913.5	0.344	86	0.275	250.11	0
C7+	0.60084403	183.48	1813.28	1.319	369.06	0.635	796.28	0.286

The accuracy and predictability of the tuned EOS can be observed by comparing the experimental and simulated values for various properties.

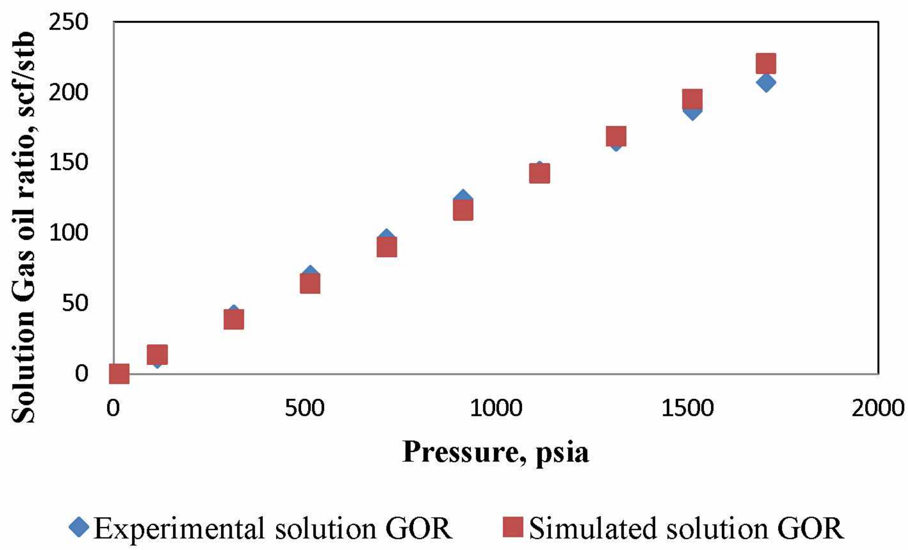

Figure 10: Experimental and simulated Gas oil ratio (GOR).

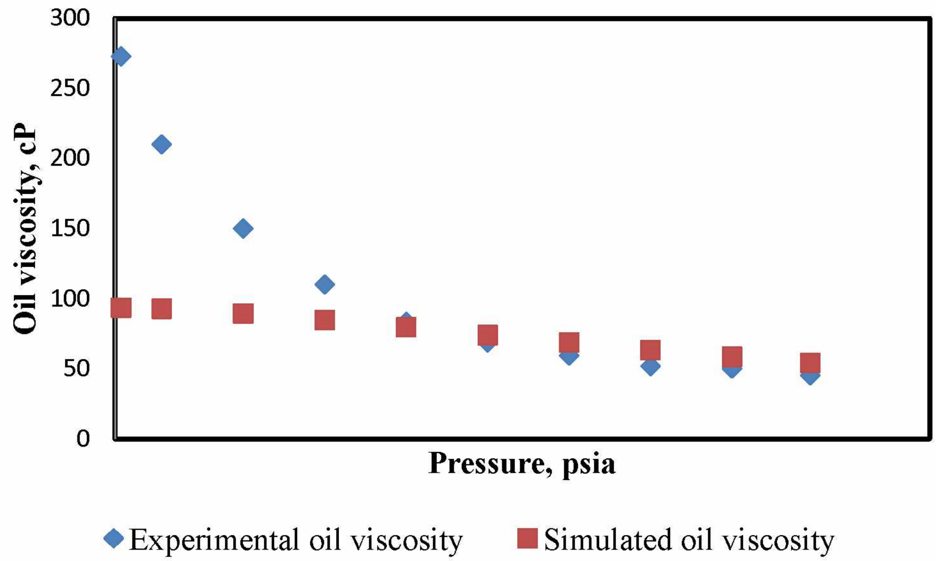

Figure 11: Experimental and simulated oil viscosity.

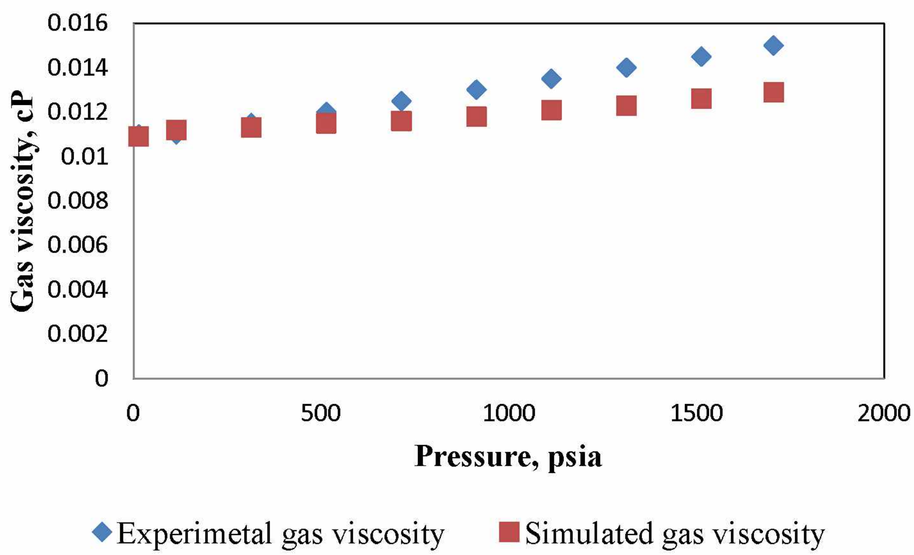

Figure 12: Experimental and simulated gas viscosity.

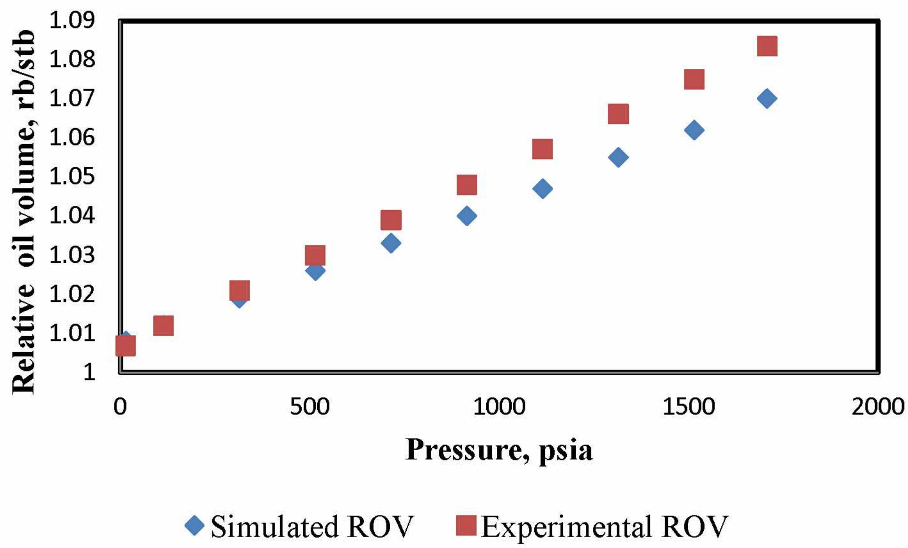

Figure 13: Experimental and simulated Relative oil volume (ROV).

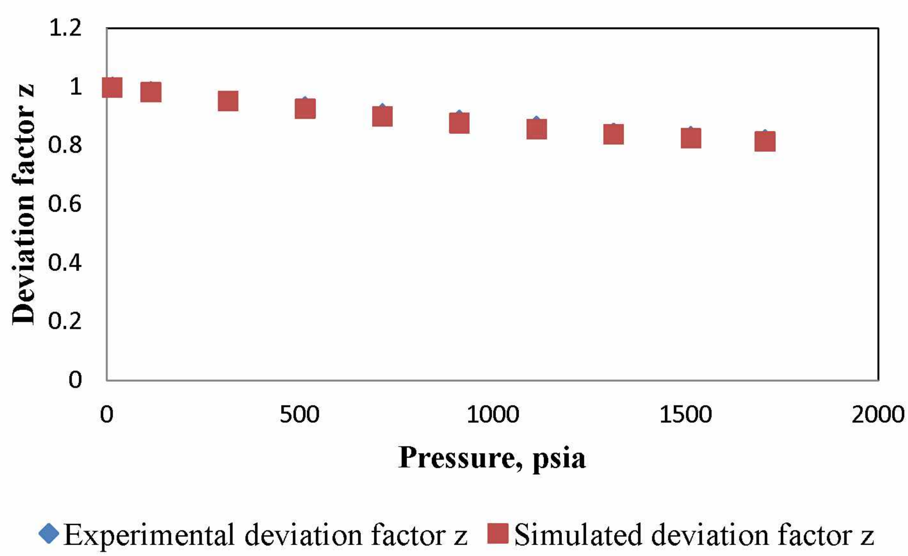

Figure 14: Experimental and simulated gas compressibility factor (z).

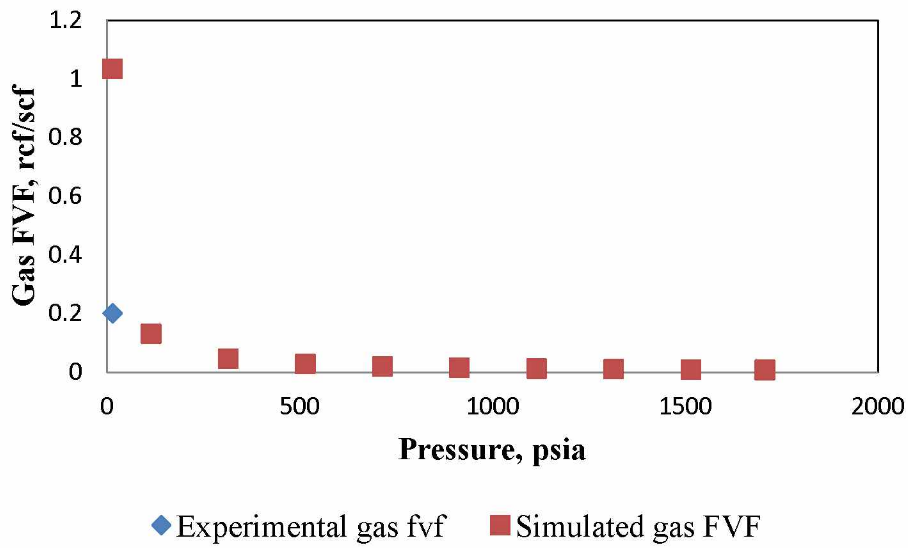

Figure 15: Experimental and simulated as formation volume factor (FVF).

4.2 Reservoir simulation without Geomechanics

Reservoir simulation is carried out in order to study the effect of bottomhole pressures, injection rates and injection pressures on waterflooding. The simulations run are the base case.

Figure 16 shows that the recovery curves for different cases are essentially identical. If a higher PV is injected, a higher recovery is obtained but the recovery trend remains the same. It can also be inferred that operating conditions do not have any effect on recovery as all the curves traces the same path.

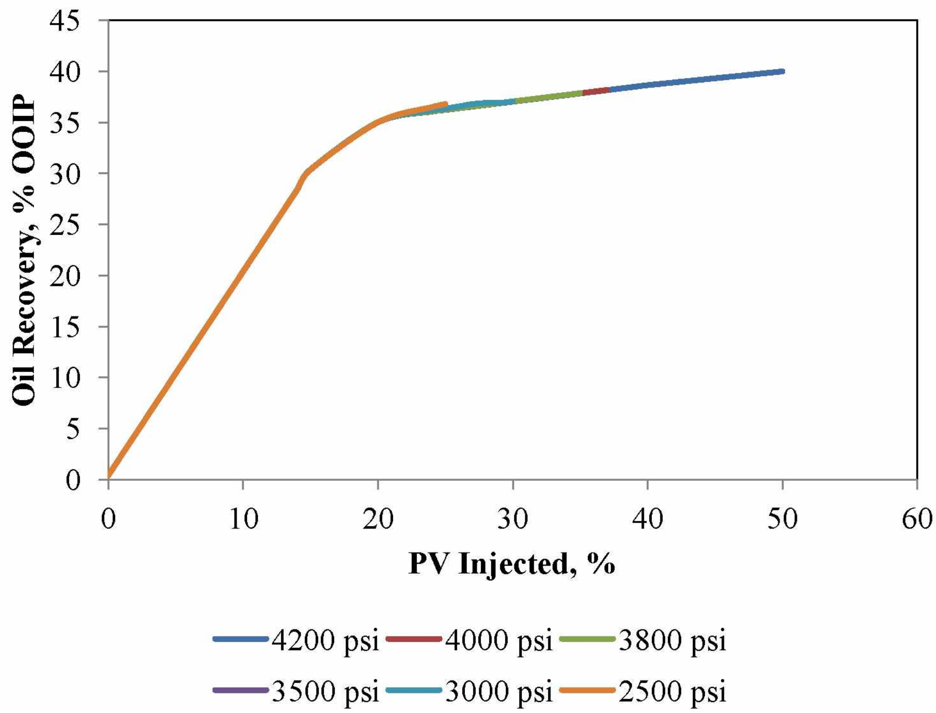

Figure 16: Oil recovery at different PV injected for various injection pressures.

Figure 17 shows that the porosity for the reservoir increases with injection at a constant producer CBHP of 1600 psi. It can be seen that the values for porosity increase with injection and then reach almost constant values. An increase in the porosity is observed due to the injection of fluid in the formation. Right now, as no geomechanics is coupled, the mechanical changes are only due to oil production. No formation failure is considered yet.

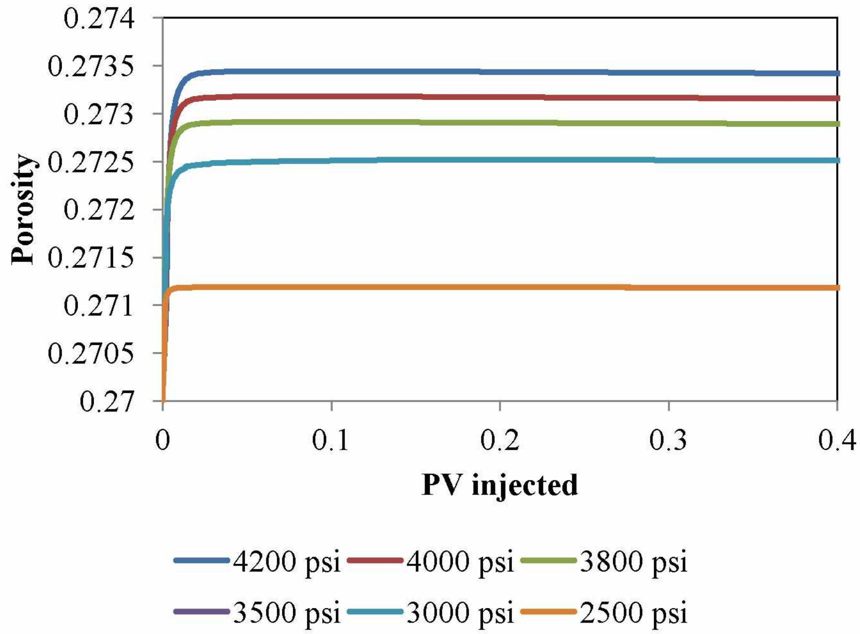

Figure 17: Porosity at different PV injected for different injector CBHP.

Subsidence is defined as downward movement of the formation. In equilibrium conditions, overburden is supported by pore pressure. When fluids are produced, the pore pressure decreases and the formation subside. Figure 18 shows that the formation doesn't subside and tend to expand due to injection. At a higher injection rate the expansion is higher. The values are negative in the graph, as the upward movement is defined as negative.

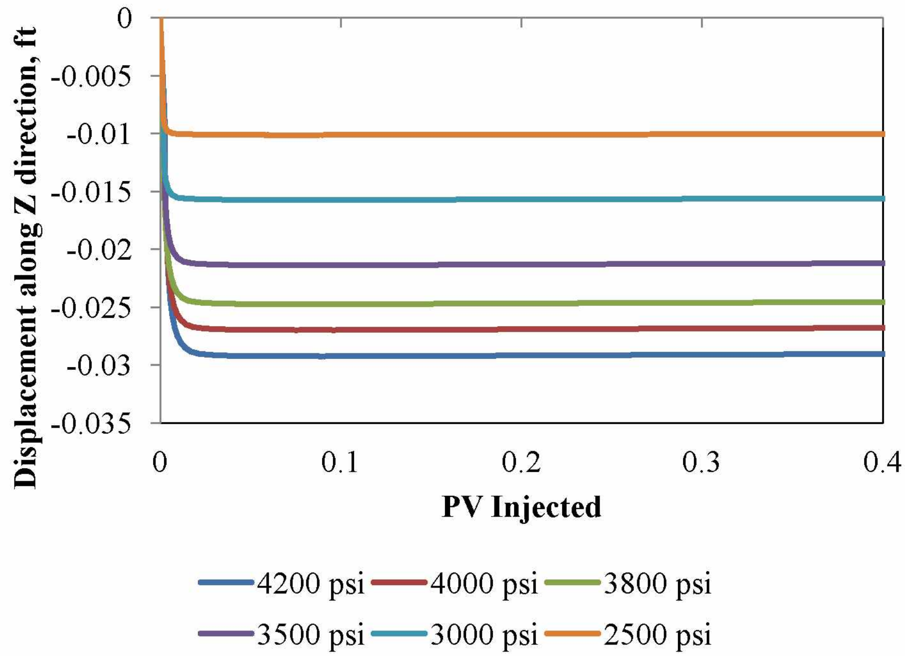

Figure 18: Displacement along Z direction (ft) at different PV injected for different injector CBHP.

4.4 Reservoir simulation with Geomechanics

Until now, when simulations are run, no importance is given to geomechanics. From now on, the geomechanics module in the CMG - Builder is used to run the simulations. Properties such as effective mean stress and yield state are given importance and the new calculated porosity, strain, and subsidence/expansion are used while producing oil. For all the scenarios when injection pressure is varied, the production pressure is kept at 1600 psi.

Geomechanics are coupled to the scenarios for waterflooding. Again, different operating pressures do not seem to cause any change in the recoveries. Recovery is only related to the PV injected. A higher PV injection leads to a higher recovery (Figure 19).

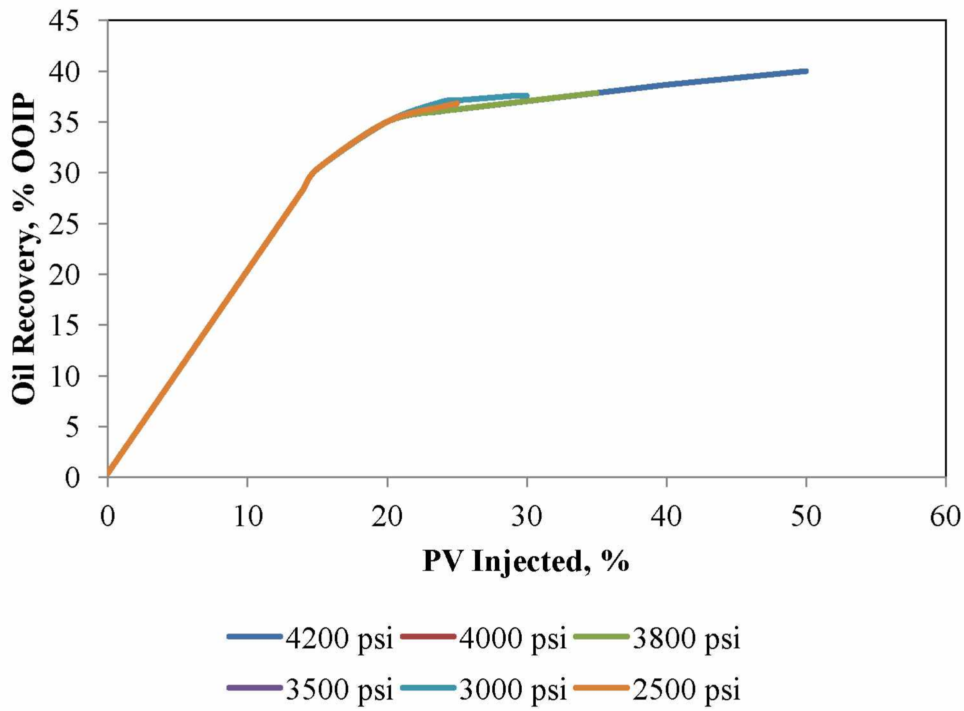

Figure 19: Oil recovery at different PV injected for various injector pressures.

Fluid flow and formation deformation (geomechanics) are coupled together in a sequential manner, meaning, the two calculations alternate while passing information back and forth. The fluid flow calculation updates the pressure and temperature and the geomechanical module updates the deformation in response. Coupling allows the user to select the particular form of porosity function for the coupling of reservoir flow equations and geomechanical calculations. When no geomechanics module is used the simulator used the original porosities and when different couplings are used the simulator recalculates the porosity based on the defined porosity evaluation methods. For coupling 0, fluid flow porosity contains no parameter that depends on deformation from geomechanics and hence the porosity value matches the original porosity values. In coupling 2 and 3, the porosity is a function of pressure, temperature and total mean stress formula. The porosities from coupling 2 and 3 only differ in their mathematical forms. The constants in coupling 2 have differential equations forms while the constants in coupling 3 have linear forms. It can be observed that both of these coupling options give similar porosity values. Throughout the simulations coupling option 2 is used. In case of coupling 1, the porosity is dependent on pressure, temperature and volumetric strain. Because of the numerical error this case couldn't be run. Further information regarding coupling can be obtained from the CMG STARS Manual.

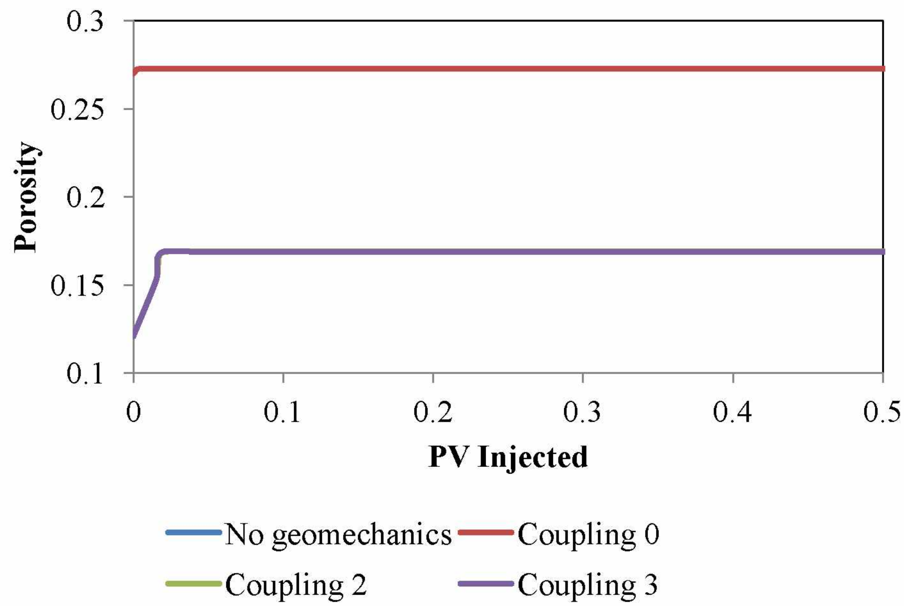

Figure 20: Porosity at different PV injected for various coupling options.

To estimate which section of the formation should be used to analyze geomechanical properties, the change in porosity, effective mean stress, volumetric strain, displacement along Z direction, and yield state vs. distance from injector is plotted. For all the plots, the injection well is kept as a reference. So 0 ft is the location of injection and the farthest away point on the distance is the location of the producer well.

From Figure 21, it seems that the closer the formation is to the injector well, the higher the volumetric strain exerted on it. A higher injection pressure when producer pressure is kept at a constant pressure of 1600 psi leads to a higher volumetric strain. Volumetric strain can be defined as the ratio of change in bulk volume to initial volume. The values are negative, as the formation is expanding.

It can be seen that extreme values are found where the formation is closest to the injector and the producer. To understand the behavior of any property, the extreme locations, i.e., the formation close to the injector and producer should be used. Other plots for effective mean stress on the formation, displacement of the formation, and porosity and yield state of the formation also show similar conclusions (Figures 21- 25).

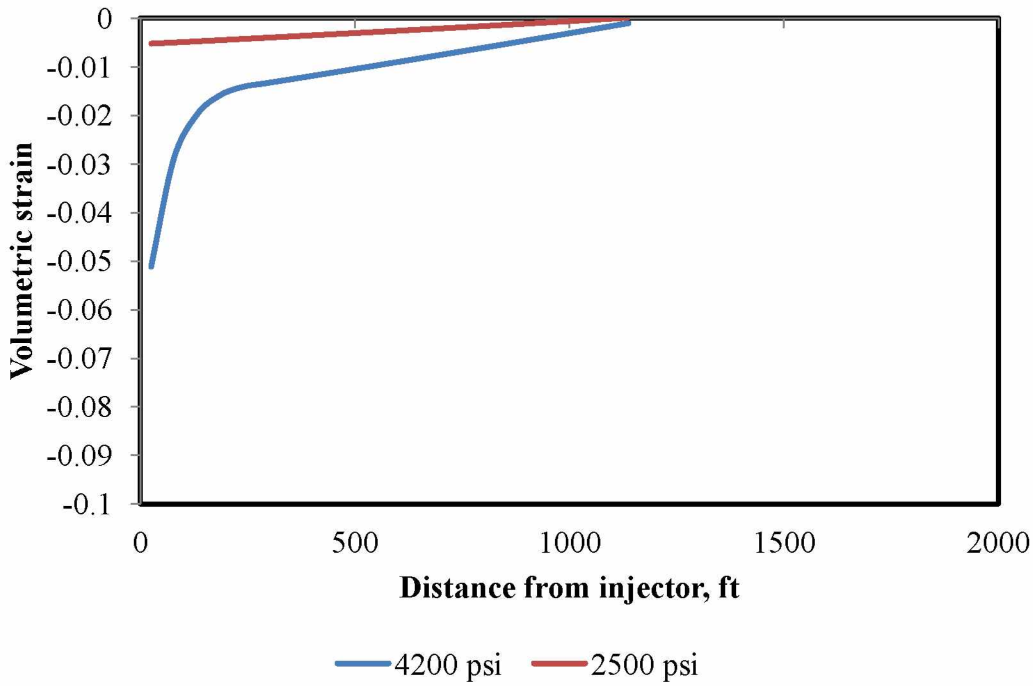

Figure 21: Change in volumetric strain with distance for injector at different pressures.

The stress values vary between 100 to 2000 psi between the elements closer to the injection well and the producer well (Figure 21). The initial stress in all the directions is maintained at 2500 psi. Once the production starts, the stress values fall from 2500 psi to as low as 50 psi. The stresses seem to be dominated by the injection pressures. The injection pressure works in opposition to the formation stresses. With an increase in pressure, there is a decrease in effective stress.

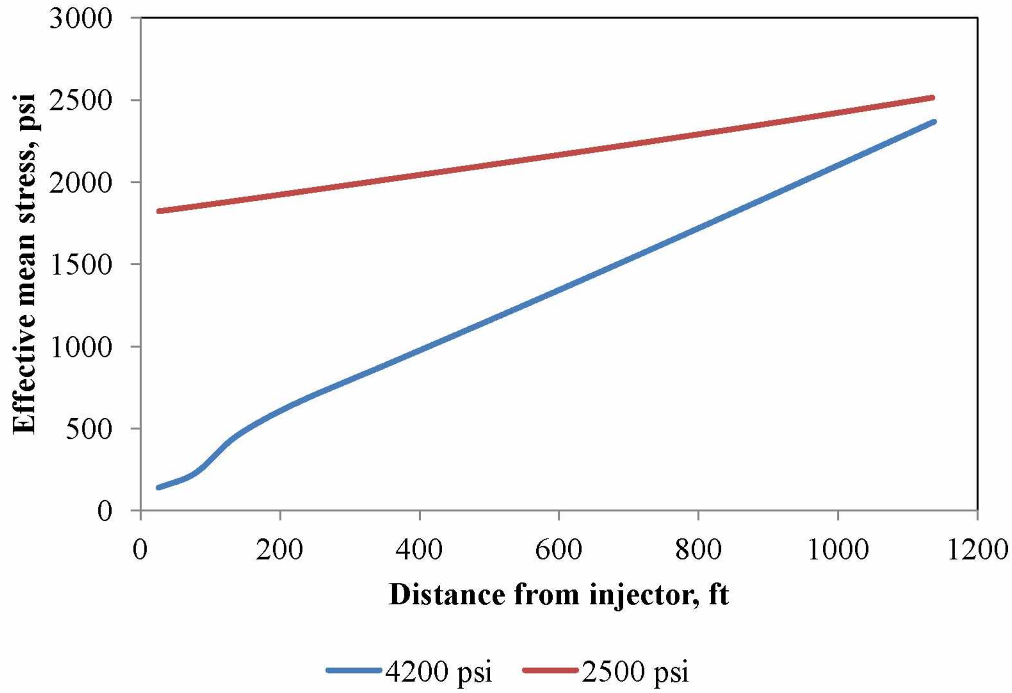

Figure 22: Change in effective mean stress (psi) with distance for injector at different pressures.

As the stresses and strains are higher near the injector wells, porosity is also observed to be higher there (Figure23). Coupling option 2 is used while calculating the porosity.

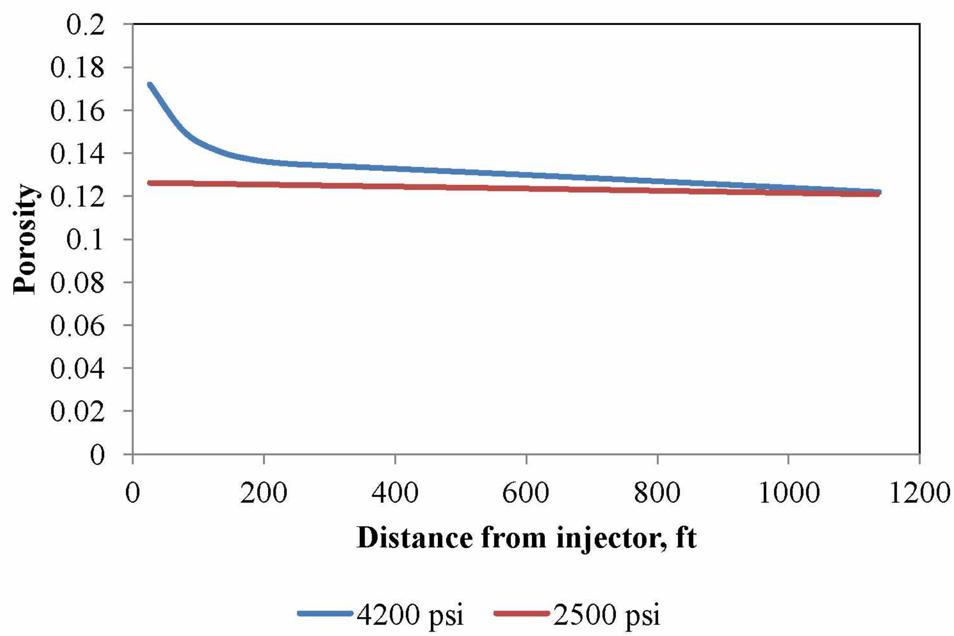

Figure 23: Change in porosity with distance for injector at different pressures.

The displacement along Z direction for the formation section closest to the injector well can be about 2 ft for an injector pressure of 4200 psi (Figure 24). A very high displacement is observed as the pressure is very high for the reservoir and can be noticed that the formation is acting plastically from the yield state curve. No such observation is made at a lower pressure. Again negative sign means that the formation is rising.

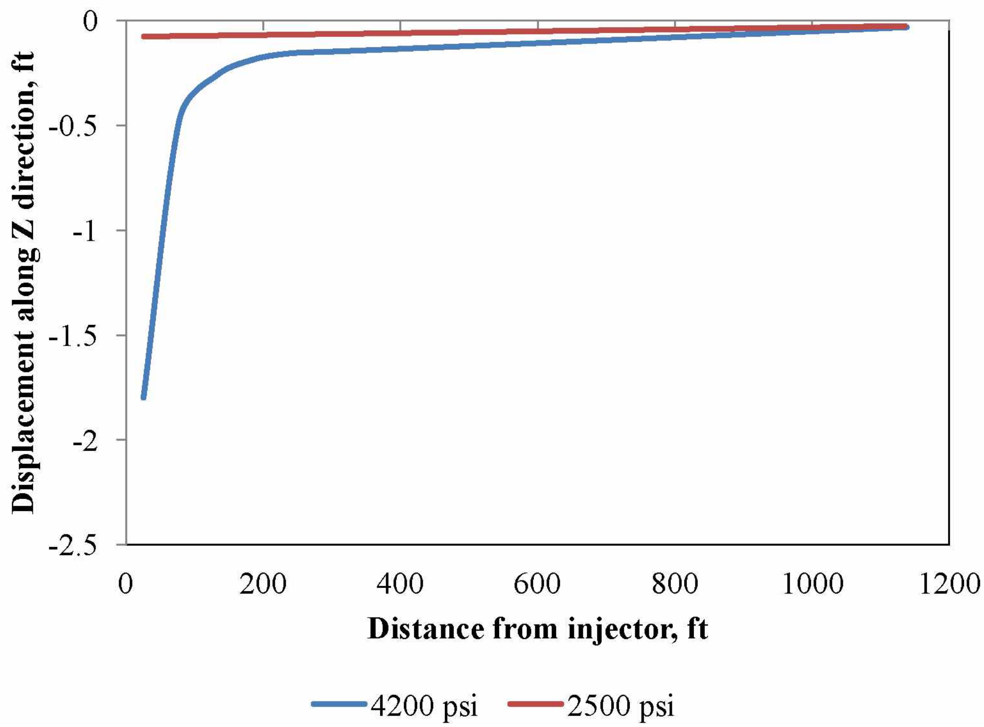

Figure 24: Displacement along Z direction (ft) with distance for injector at different pressures.

From the examination of the yield state, it is observed that few blocks are flagged as 0 and few have numbers associated with them. The elements with a zero value signify that they have not reached the failure criteria and crossed from elastic behavior into plastic. The elements flagged as 1 have reached the failure criteria. Other values in between 0 and 1 are not important. Yield state is important as it directly signifies the probability of sand production. Once an element has yielded, it has a higher probability to be produced as sand. From Figure 25, it seems that the formation closest to the injector wells has a higher probability of failing and producing sand. It can be seen that at an injection of 4200 psi the formation closer than 400 ft from the injector well fails. After 400 ft the formation doesn't fail and hence the blocks are flagged as 0.

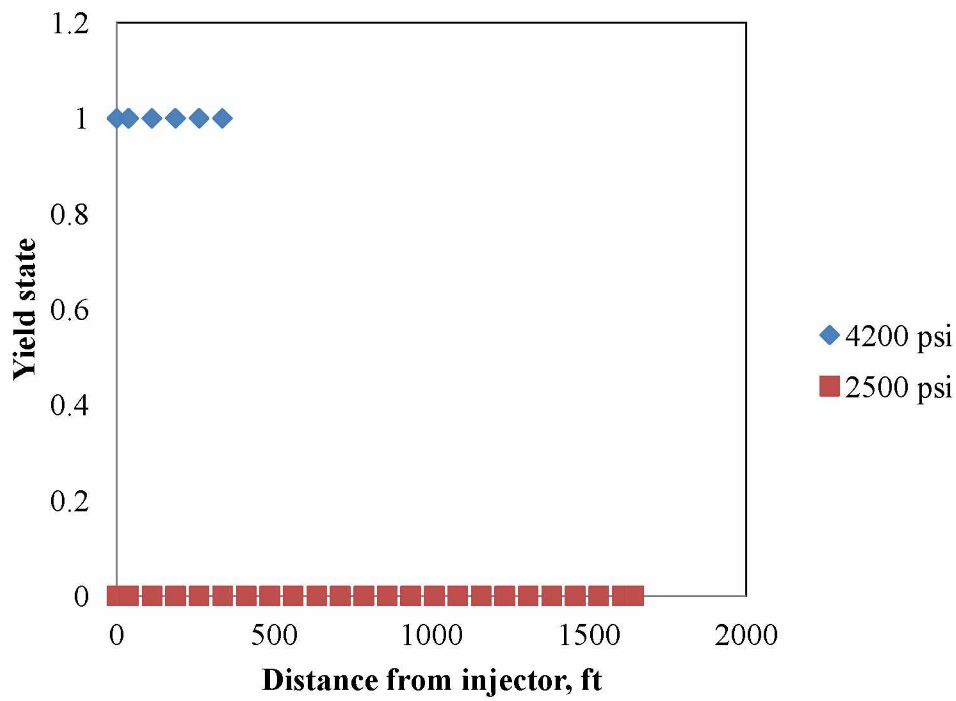

Figure 25: Change in yield state with distance for injector at different pressures.

To analyze the geomechanical properties and how they behave, the formation closest to injector well is observed.

By analyzing the effective mean stresses, it can be observed that injection pressure acts on the formation against the initial stress of 2500 psi. As the injection starts, the stress decreases drastically, and after that, it maintains a constant value. At very high injection pressures, the effective mean stress falls as much as 10 psi (Figure 26). Such drastic decrease in the mean stress also leads to a tendency to produce sand. At a lower injection pressure, the change is not very drastic, and the effective mean stress stays in a safer region. In Figure 27, it can be observed that when constant injection rates are used as the operating parameters, the effective means stress decreases with a continuous injection and after some time becomes constant. To understand this behavior bottomhole pressure of the well should be observed. It is seen that the bottomhole pressure increases as soon as injection is started and after some time it attains a constant value (Figure 32). And it is understood that injection pressure acts against the effective mean stress.

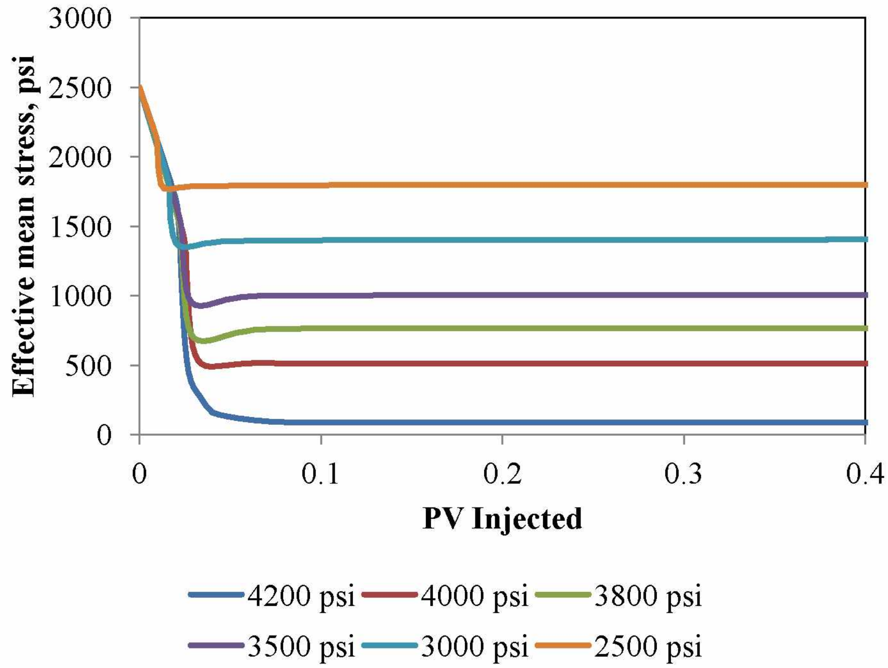

Figure 26: Effective mean stress (psi) at different PV injected for different injector CBHP.

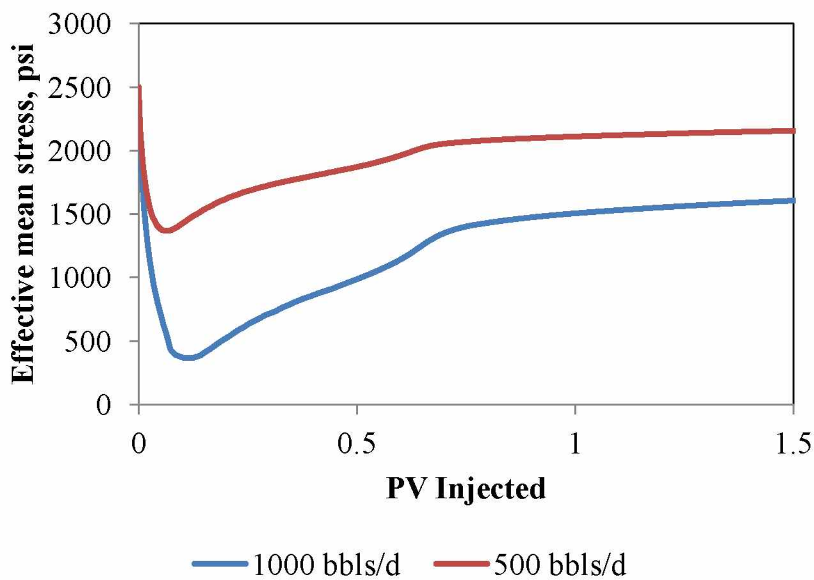

Figure 27: Effective mean stress (psi) at different PV injected for different injection rates.

Now that coupling 2 is used, as the stress change, the porosity due to geomechanics also changes. With a decrease in stress, porosity increases. Once the stresses stabilize, the porosity value also stabilizes. Significant changes in porosity are observed for higher injection parameters

(Figure 28 and 29). A higher injection pressure leads to more deformation, and higher porosity values are obtained at higher injection parameters.

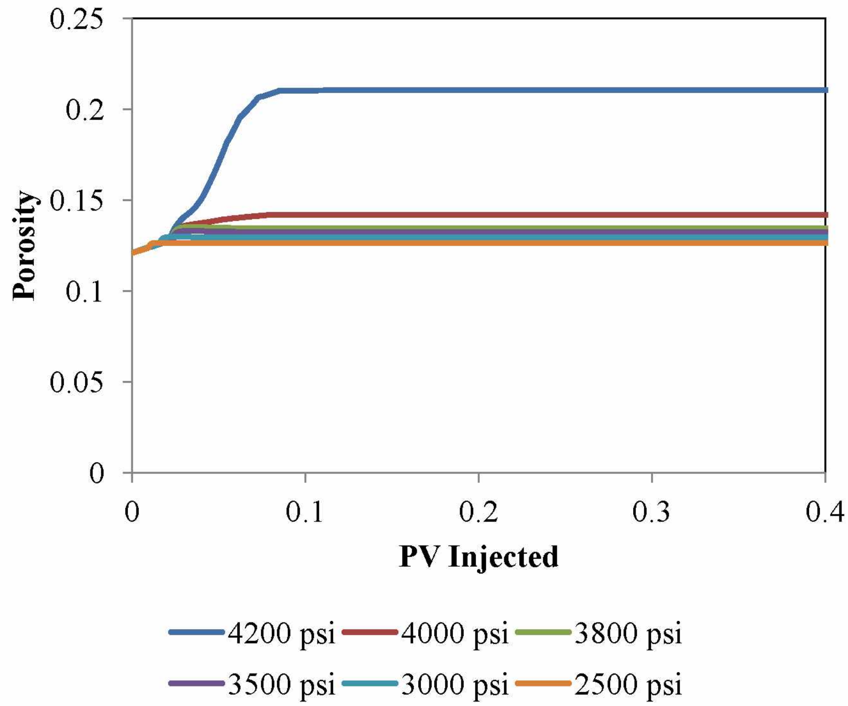

Figure 28: Porosity at different PV injected for different injector CBHP.

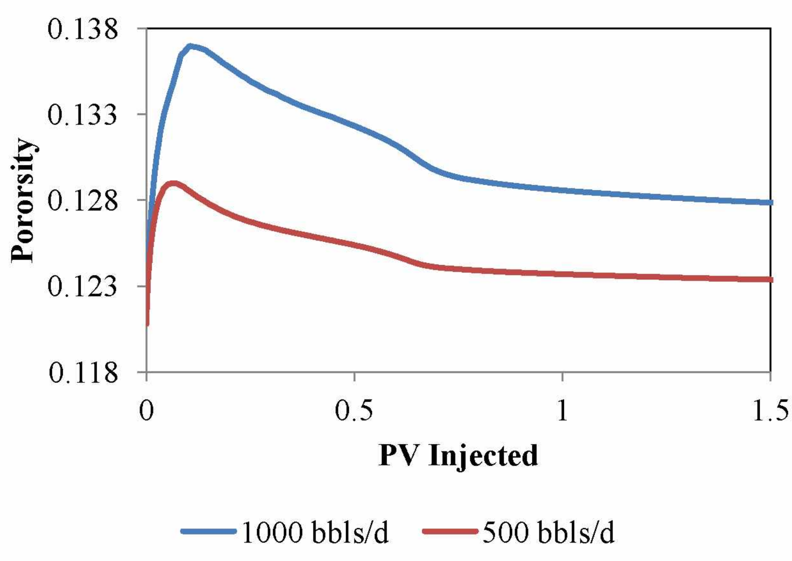

Figure 29: Porosity at different PV injected for different injection rates.

At a very high injection pressure, a displacement along Z direction can be as much as 2 ft for extreme cases (Figure 30). The typical values range from 0.1 to 0.4 ft. The extreme value for 4200 psi is obtained as the injection pressure exceeds the failure criteria. Negative sign for the displacement signifies that the formation is rising. Similarly, at an injection rate 500 bbls/day this displacement can be 0.1 ft, while 0.8 ft at a higher injection rate.

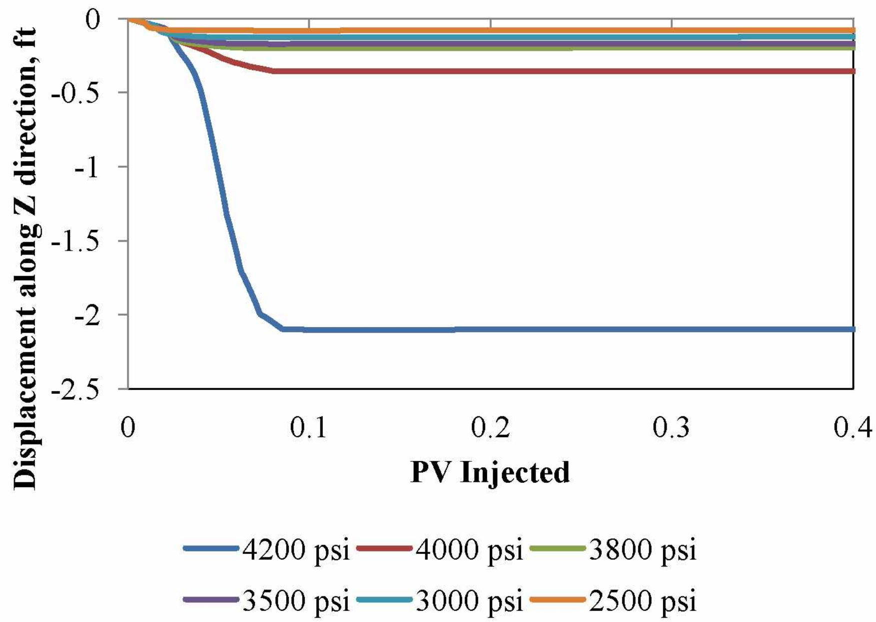

Figure 30: Displacement along Z direction (ft) at different PV injected for different injector CBHP.

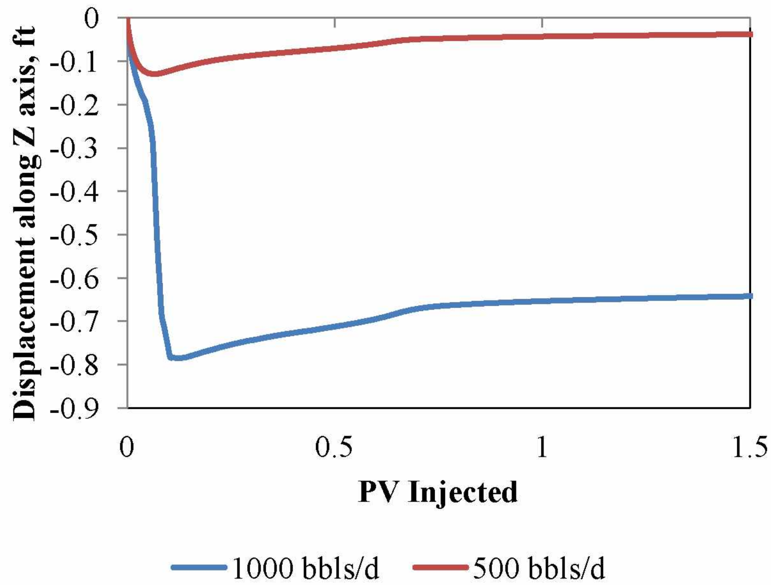

Figure 31: Displacement along Z direction (ft) at different PV injected for different injector CBHP.

From Figure 32, it can be seen that the curve for displacement along Z direction seems like a mirror image of the bottomhole pressure. Because the injection rates are kept constant the well bottomhole pressure first increases and then decreases and attains a constant value. The bottomhole behavior is due to the water and oil mobility. Water has a higher mobility than oil. During the start of the injection the water is trying to displace oil. Hence the bottomhole pressure increases but soon water starts to fill more area and after some time injection starts acting on water. Water has a lower compressibility than oil and hence the bottomhole pressure starts to decrease. After some time bottomhole pressure attains a constant value. As seen earlier, higher the bottom hole pressure is, higher will be the displacement along Z direction.

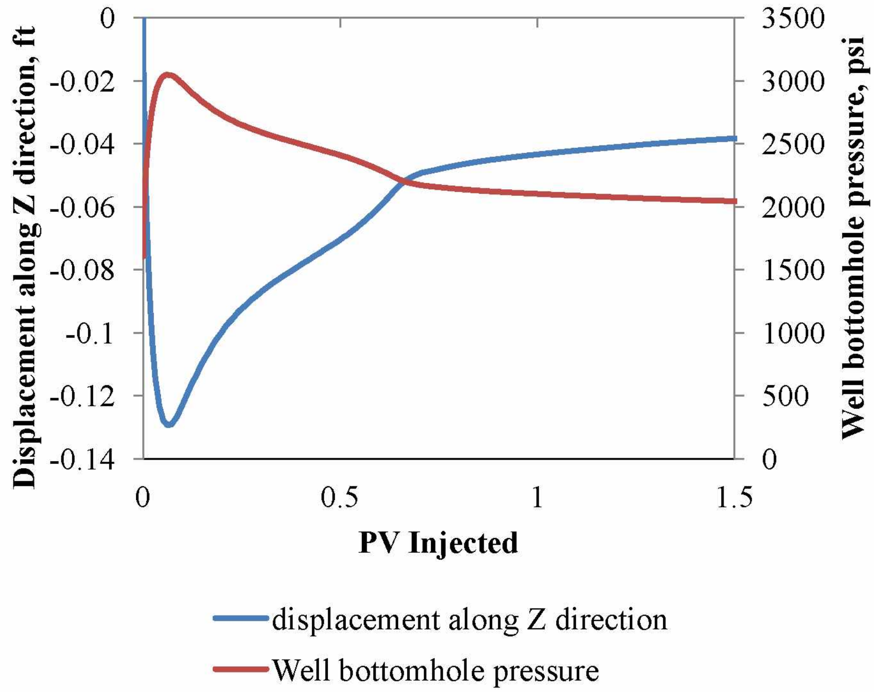

Figure 32a: Displacement along Z direction and well BHP at different PV injected when constant injection rate is 500 bbls/d.

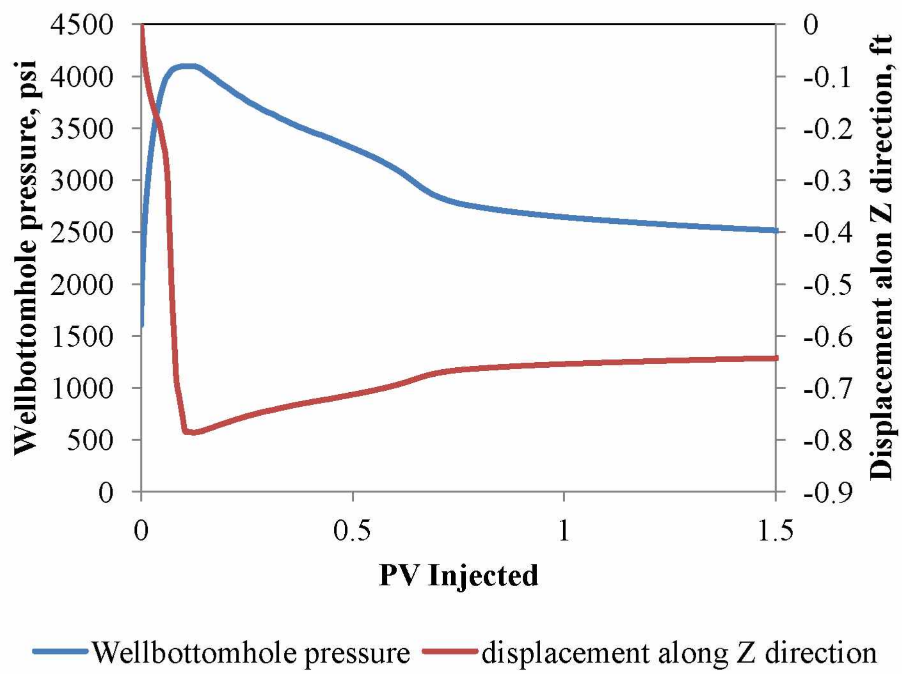

Figure 32b: Displacement along Z direction and well BHP at different PV injected when constant injection rate is 1000 bbls/d.

Movement of the formation leads to a change in bulk volume. Bulk volume change can be measured in terms of volumetric strain. Volumetric strains as much as 0.09 are measured for injection wells at 4200 psi (Figure 33). Lower values are obtained for volumetric strains for various injection rates as compared to scenarios when bottomhole pressure is used as the operating parameter (Figure 34).

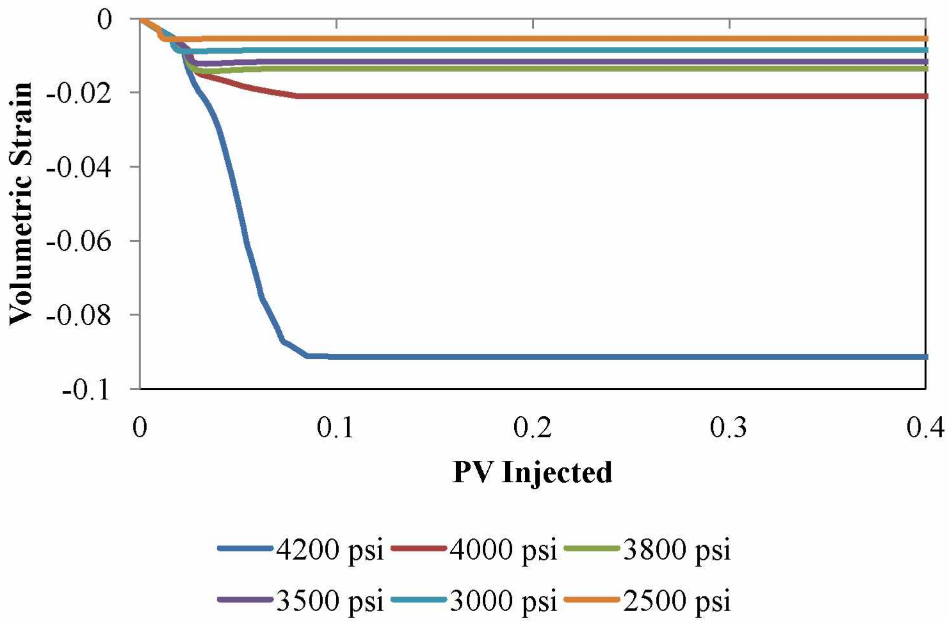

Figure 33: Volumetric strain at different PV injected for different injector CBHP.

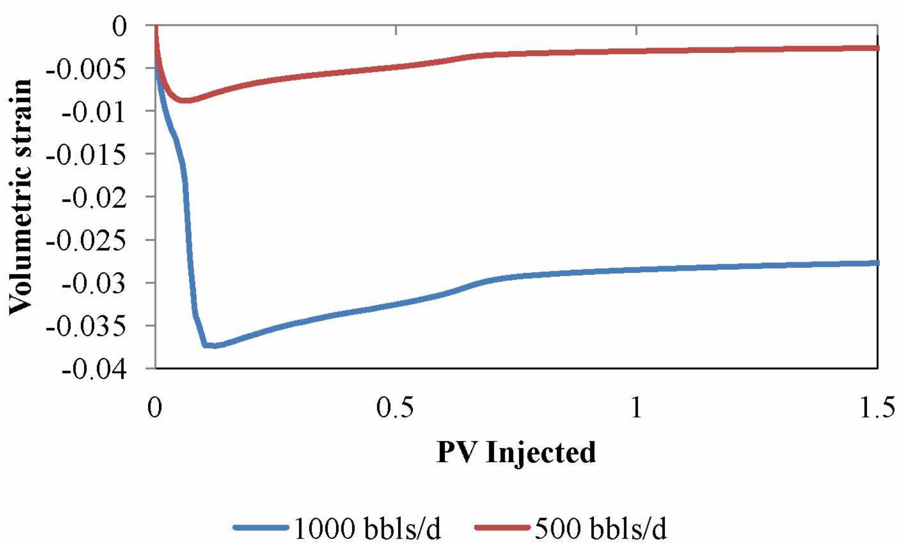

Figure 34: Volumetric strain at different PV injected for different injection rates.

A value equal to 1 signifies that the formation is in the plastic state and a value of 0 means the formation is in the elastic region. Yield state is important because it indicates the probability of sand production. Once an element has yielded (plastic region), it has a higher probability to be produced as sand. Any value between 1 and 0 is not very significant. The closer the value is to 1, the higher the likelihood that the formation might reach the plastic state. It can be observed that elements have a tendency to yield when the injection pressures are 4200 psi and 4000 psi (Figure 29). It can be concluded that for safe sand-less production, the injection pressure should not exceed 3800 psi. Similarly from Figure 36, it can be concluded that if injection rates are used as operating parameter, the rates should be kept lower that 1000 bbls/day.

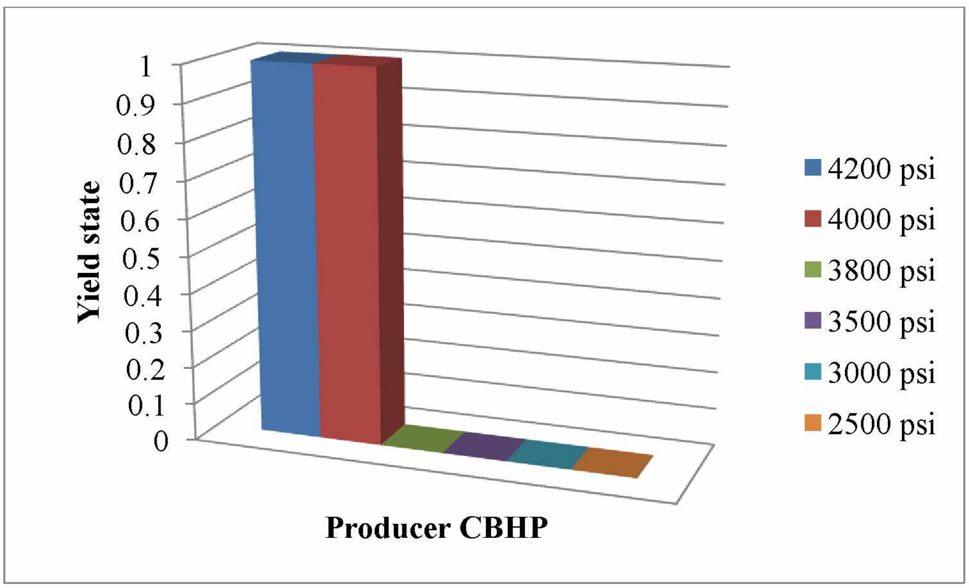

Figure 35: Yield state at 0.05 PV injected for different injector CBHP.

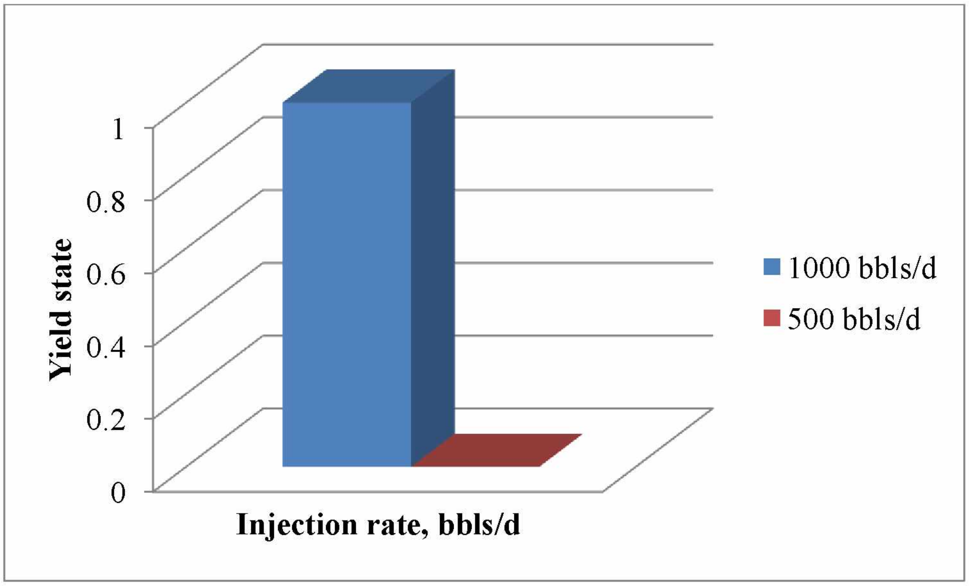

Figure 36: Yield state at 0.06 PV injected for different injection rates.

4.5 Comparison between cases with and without Geomechanics

To understand how much the values are off when geomechanics is not coupled, plots for different properties are made. The plots are made at the maximum and minimum injection and production pressures.

When oil rates are compared in Figure 36, it is observed that a higher oil production seems to be achieved when no geomechanics is coupled. It can also be assumed that if geomechanics is controlled, better production can be realized.

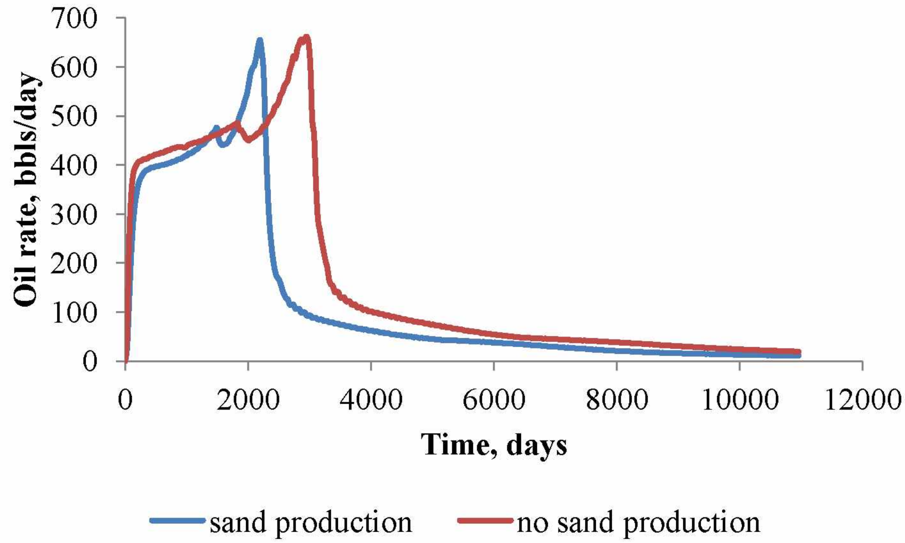

Figure 36: Oil rate for waterflooding when injection pressure is at 3800 psi and producer pressure is at 1600 psi.

It can be observed that higher the injection pressure, the greater the difference between cases coupled with geomechanics and uncoupled. At an injection pressure of 4200 psi, the difference in the cases can be as much as 2000 psi (Figure 37). Neglecting to consider this difference could cause well integrity issues in the later stages of a well's life.

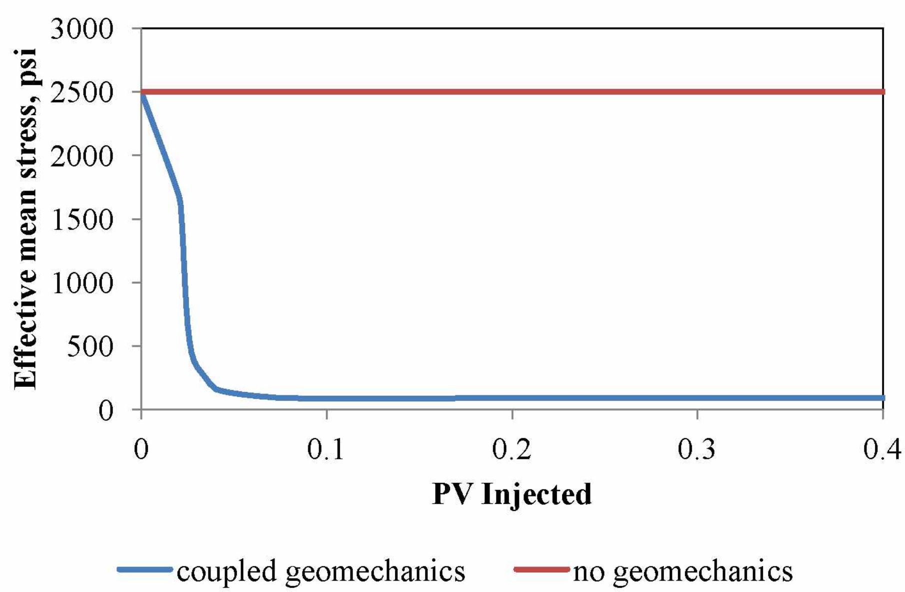

Figure 37: Effective mean stress (psi) when injection well pressure is 4200 psi.

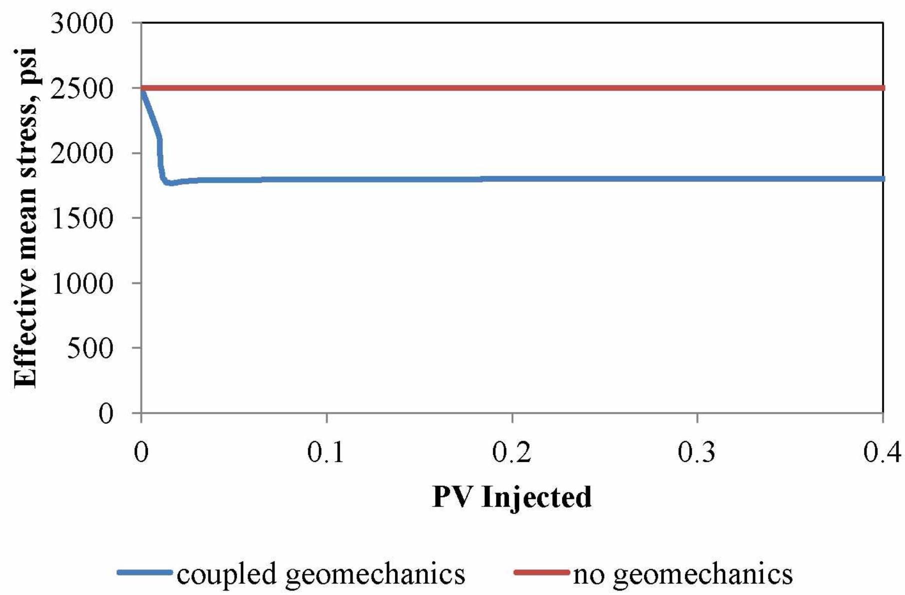

Figure 38: Effective mean stress (psi) when injection well pressure is 2500 psi.

When geomechanics is not coupled, the displacement of formation due to production/injection is calculated to be as low as 0.01 ft. With regard to the movement of formation, coupling geomechanics in the reservoir model should be must for unconsolidated reservoirs.

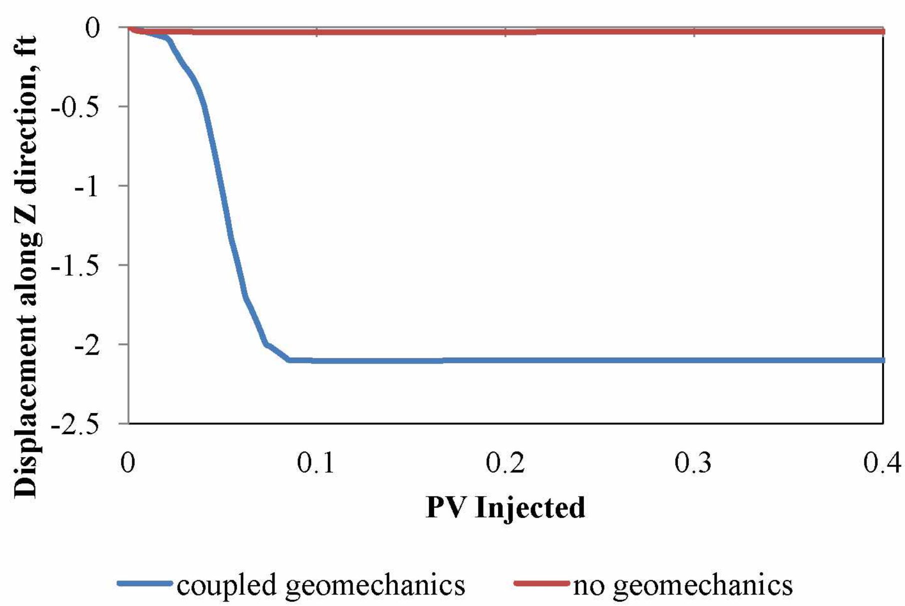

Figure 39: Displacement along Z direction (ft) when injection well is at 4200 psi.

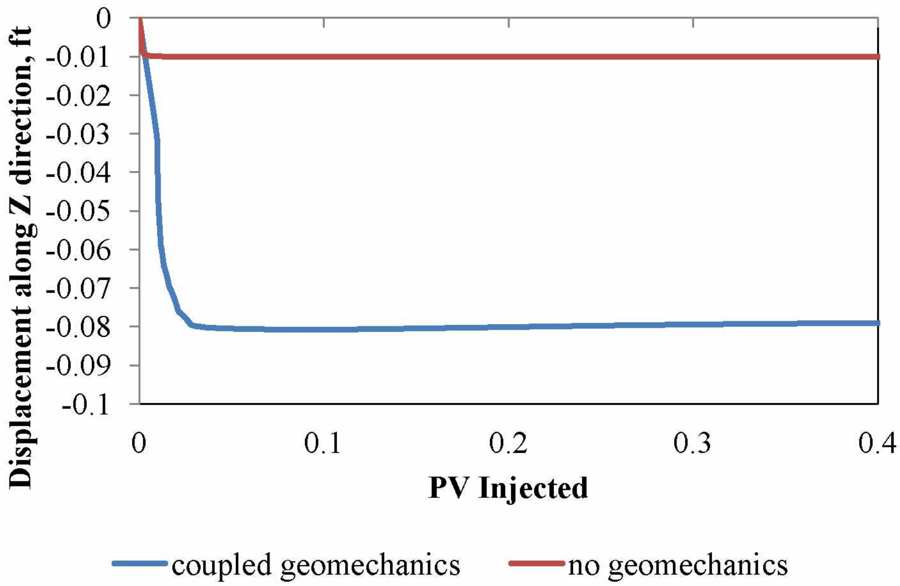

Figure 40: Displacement along Z direction (ft) when injection well is at 2500 psi

If geomechanics is not considered, the calculated volumetric strain on the formation is very low as it is dependent on the displacement. Such a variation between reality and simulation can lead to well integrity issues.

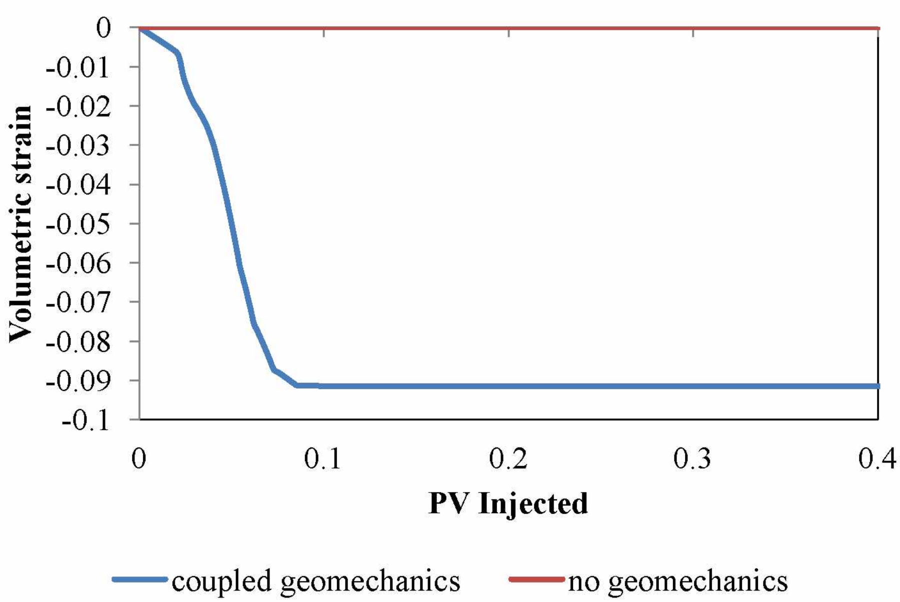

Figure 41: Volumetric strain when injector well pressure is 4200 psi.

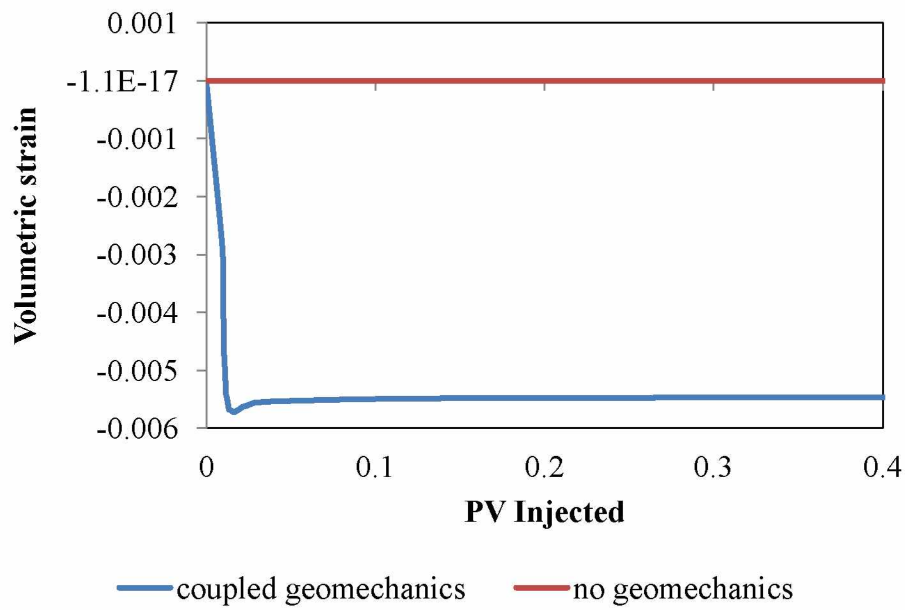

Figure 42: Volumetric strain when injector well pressure is 2500 psi.

The importance of understanding geomechanics becomes crucial when the formation is known to have sand production issues. If geomechanics is not coupled, there is no way to know whether the element is yielding or not. If an element is yielding, there is a very high probability that it will be produced as sand. For sand-free production, it is suggested that operating parameters are used such that no element yields.

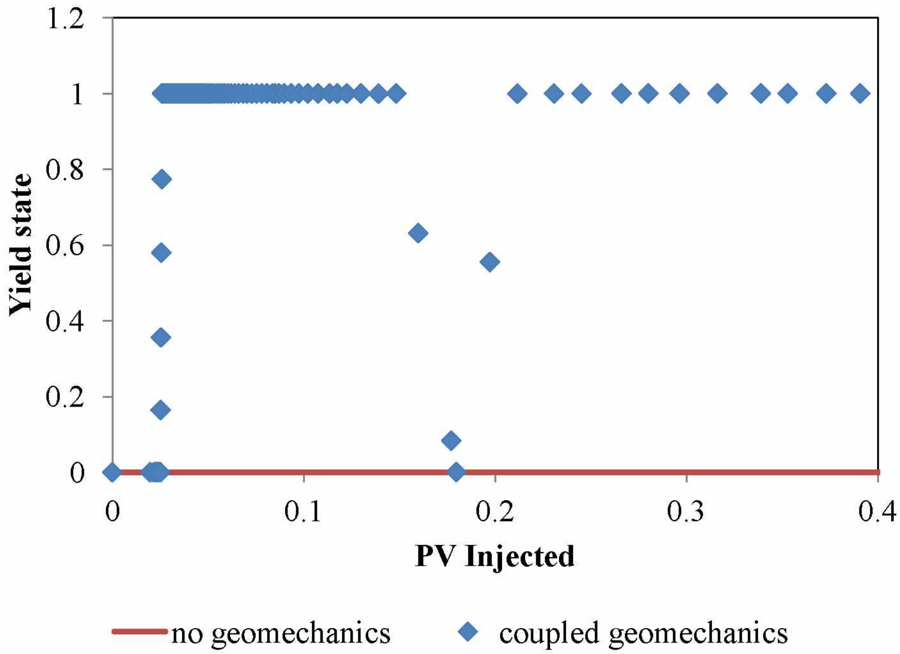

Figure 43: Yield state when injector well pressure is 4200 psi.

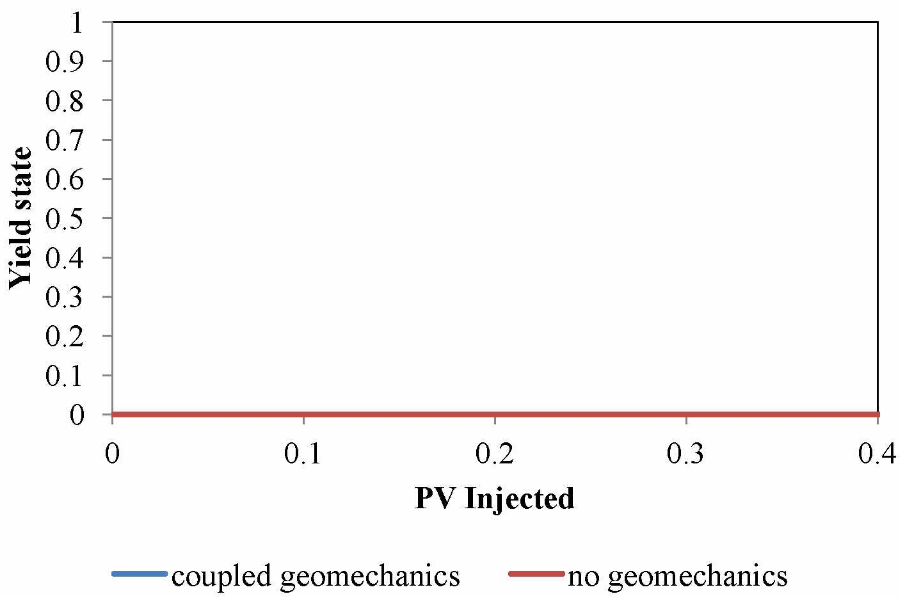

Figure 44: Yield state when injector well pressure is 2500 psi.

4.6 Effect of injection/production pressure

4.6.1 Displacement along Z direction

In Figures 45 and 46, graphs between pressures and displacement of formation along Z direction are plotted. For various injection pressures there seems to be no trend present. It can be seen that at higher injection pressures, higher displacement is observed. However, in the case of different producer CBHP, it can be seen that higher drawdown leads to lower displacement along Z direction (Figure 45). As at a higher production CBHP lesser fluids are produced and leads to more fluid accumulation in the formation leading to a rise in it. Negative sign denotes rise in the formation.

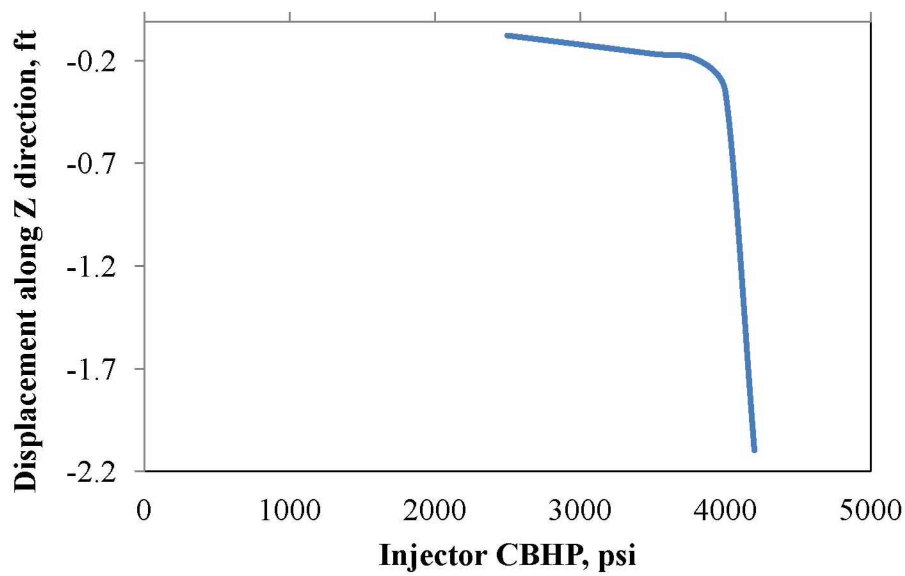

Figure 45: Displacement along Z direction with change in injector CBHP for waterflooding.

4.6.2 Yield state

There seems to be no correlation between yield and operating pressures. However, from the plots of yield state versus pressure, it can be concluded that there exists a pressure beyond which the formation will always yield.

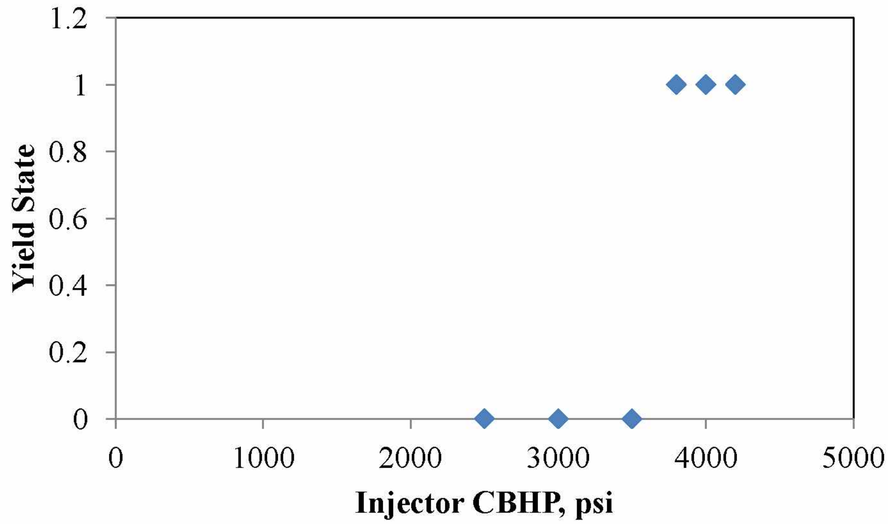

Figure 47: Change in yield state with change in injector CBHP for waterflooding.

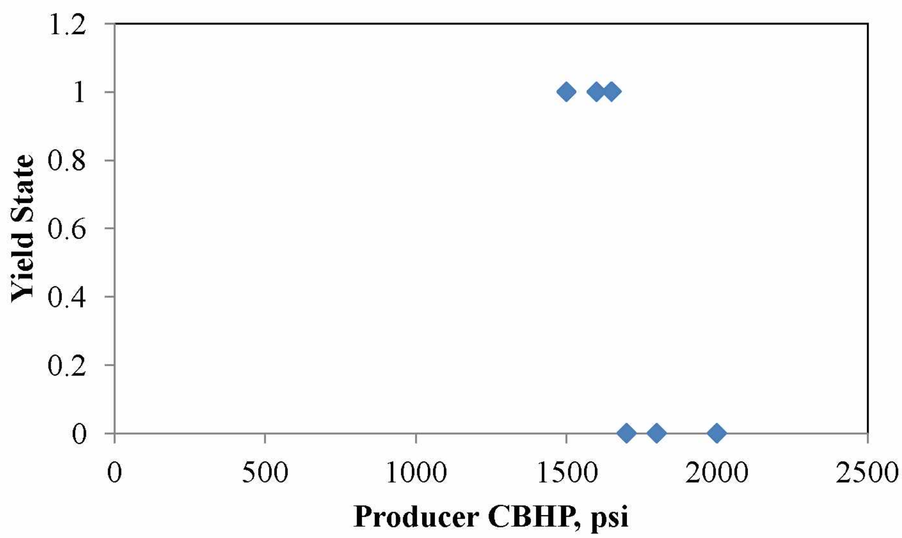

Figure 48: Change in yield state with change in producer CBHP when injector is maintained at 3800 psi.

Chapter Five

Conclusions and Recommendations

5.1 Conclusions

A maximum of 40% difference is found between the oil rates for cases when no geomechanics is coupled and when geomechanics is coupled. This difference in oil production is due to the change in geomechanical properties such as stress and strain. These stress and strain values change due to continuous oil production. Even if the reservoir oil production is supported by pressure maintenance through injection of fluids, with time, geomechanical properties change.

The formation closest to the injection well or producer well seems to be affected most by injection and production. For various scenarios, the volumetric strain caused can be 0.1 - 0.12. The change in the effective mean stress from the initial effective mean stress can be 2000 - 2400 psi. Geocorrection to porosity values is found to be 0.12 - 0.25. Displacement along Z direction caused due to geomechanics is about 2 - 2.75 ft.

To understand the behavior and trends of subsidence/expansion, properties such as yield state, effective mean stress, and pressure should be observed. Trends in porosity can be understood from yield state and effective mean stress. Effective mean stress is directly related to the pressures in the formation. Trends in volumetric strain can be understood by looking at the displacement of the formation. Yield state is the most important property that shouldn't be ignored. As the yield state can be used to understand whether the formation is acting elastically or plastically based on Mohr - Coulomb criteria. If the formation has failed the criteria, there is a higher chance that it might be produced as sand.

It is understood that if geomechanics is not considered, a lot of important properties such as stress changes, volumetric strain, and yield state are neglected. Neglecting these properties can lead to well integrity issues.

Understanding geomechanical properties can help solve issues related to well integrity and sanding. In the case studied, the injection pressure for yield-free production is found to be lower than 3800 psi, and producer well pressure to be higher than 1600 psi. And if injection rates are used as the operating parameter, it should be maintained at a rate which is lower than 1000 bbls/d.

5.2 Recommendations

Regarding the simulations run for the West Sak reservoir, the tuned EOS model is able to simulate results similar to experimental values. For better compositional models, other data such as separator tests and slim tube tests should be incorporated.

The used relative permeability data is very old. For better data, new core-flooding experiments should be performed. The model built to study geomechanics is homogeneous in nature. It is recommended that heterogeneity of the reservoir is considered when making a decision regarding operating parameters.

This study can be further improved by analyzing how much profit can be realized by controlling the effects of geomechanics. As there was no data available regarding the cost of the equipment and techniques, no such study is conducted.

References

Alam, M. M., Hjuler, M. L., Christensen, H. F., & Fabricius, I. L. (2011, January 1). Impact of Supercritical CO2 Injection on Petrophysical and Rock Mechanics Properties of Chalk: An Experimental Study on Chalk from South Arne Field, North Sea. Society of Petroleum Engineers. doi:10.2118/147056-MS

AOGCC Pool Statistics, 2004. http://doa.alaska.gov/ogc/annual/annindex.html.

Bakshi, A. K., 1991. Computer Modeling of CO2 Stimulation in the West Sak reservoir, University of Alaska Fairbanks, MS Thesis.

Bakshi, A.K., Ogbe, D.O., Kamath, V.A, Hatzingnatiou, D.G. 1992. Feasibility Study of CO2 Stimulation in the West Sak Field, Alaska. Presented at the Western Regional Meeting. SPE 24038. California

Bennion, D. B., Thomas, F. B., Bietz, R. F., & Bennion, D. W. (1998, December 1). Underbalanced Drilling: Praises and Perils. Society of Petroleum Engineers. doi:10.2118/52889-PA

Benzagouta, M. S., & Amro, M. M. (2009, January 1). Pressure and Temperature Effect on Petrophysical Characteristics: Carbonate Reservoir Case. Society of Petroleum Engineers. doi:10.2118/126045-MS

BP Statistical Review of World Energy June 2013, BP plc. (June 2013)

Burton, R. C., Chin, L., Davis, E. R., Enderlin, M. B., Fuh, G.-F., Hodge, R. M. Petersen, S. D. (2005, January 1). North Slope Heavy-Oil Sand-Control Strategy: Detailed Case Study of Sand-Production Predictions and Field Measurements for Alaskan Heavy-Oil-Multi-Lateral Field Developments. Society of Petroleum Engineers. doi:10.2118/97279-MS

Carlson, M. (2003, June 1). SAGD and Geomechanics. Petroleum Society of Canada. doi:10.2118/03-06-DAS

Chiaramonte L., Zoback M., Friedman J et al. 2011. Fracture characterization and fluid flow simulation with geomechanical constraints for a carbon dioxide EOR and sequestration project Teapot Dome Oil Field, Wyoming, USA, Energy Procedia, Volume 4, Elsevier, p. 3973-3980.

CMG - STARS Manual, 2014.

Coberly, C. J., & Wagner, E. M. (1938, August 1). Some Considerations in the Selection and Installation of Gravel Pack for Oil Wells. Society of Petroleum Engineers. doi:10.2118/938080-G

Collins, P. M. (2007, August 1). Geomechanical Effects on the SAGD Process. Society of Petroleum Engineers. doi:10.2118/97905-PA

Erwin, M. D., & Ogbe, D. O. (2005, January 1). Predicting Openhole Horizontal Completion Success on the North Slope of Alaska. Society of Petroleum Engineers. doi:10.2118/97121-MS

Fakcharoenphol, P., Charoenwongsa, S., Kazemi, H., & Wu, Y.-S. (2012, January 1). The Effect of Water Induced Stress to Enhance Hydrocarbon Recovery in Shale Reservoirs. Society of Petroleum Engineers. doi:10.2118/158053-MS

Geehan, T., Deckert, S. L., Johnson, K., & Arnold, W. T. (1999, January 1). Use of Resin-Coated Proppant to Control Shallow, Low-Temperature Unconsolidated Sands. Society of Petroleum Engineers. doi:10.2118/54631-MS

Gutierrex, M., & Lewis, R. W. (1998, January 1). The Role of Geomechanics in Reservoir Simulation. Society of Petroleum Engineers. doi:10.2118/47392-MS

Hall, C. D., & Harrisberger, W. H. (1970, July 1). Stability of Sand Arches: A Key to Sand Control. Society of Petroleum Engineers. doi:10.2118/2399-PA

Hallam, R. J., Piekenbrock, E. J., Abou-Sayed, A. S., Garon, A. M., Putnam, T. W., Weggeland, M. C., & Webb, K. J. (1992, September 1). Resource Description and Development Potential of the Ugnu Reservoir, North Slope, Alaska. Society of Petroleum Engineers. doi:10.2118/21779-PA

Hill, K. E. (1941, January 1). Factors Affecting The Use Of Gravel In Oil Wells. American Petroleum Institute.

Jonathan Bellarby, *Well Completion design*, First edition, Elsevier, Oxford, 2009.

Khodaverdian, M. F., Sorop, T., Postif, S. J., & van den Hoek, P. J. (2009, January 1). Polymer Flooding in Unconsolidated Sand Formations: Fracturing and Geomechanical Considerations. Society of Petroleum Engineers. doi:10.2118/121840-MS

King, M.J. and Mansfield, M. 1999. Flow Simulation of Geologic Models. *SPE Res Eval & Eng* **2** (4):351–367. SPE-57469-PA. http://dx.doi.org/10.2118/57469-PA.

King R. F. Drilling sideways - a review of horizontal well technology and its domestic application. Energy Information Administration. April 1993. http://www.eia.gov/pub/oil_gas/natural_gas/analysis_publications/drilling_sideways_well_technology/pdf/tr0565.pdf

Kocabas, I. (2004, January 1). An Analytical Model of Temperature and Stress Fields During Cold Water Injection into an Oil Reservoir. Society of Petroleum Engineers. doi:10.2118/88762-MS

Labuz F. J. (2012, November 1). Mohr - Coulomb Failure Criterion. Journal of Rock mechanics and rock engineering. Vol. 45, Issue 6, pp 975-979. http://link.springer.com/article/10.1007%2Fs00603-012-0281-7

Li, P., & Chalaturnyk, R. J. (2003, September 1). Discussion of "SAGD and Geomechanics." Petroleum Society of Canada. doi:10.2118/03-09-discussion

Loughead, D.J. and Saltularoglu, M. 1992. Lloydminster Heavy Oil Production Why so Unusual? Paper presented at the Annual Heavy Oil and Oil Sands Technology Symposium, Calgary, 11 March.

McCaffrey, W.J., Bowman, R.D. 1991. Recent Successes in Primary Bitumen Production. Paper presented at 8th Ann. Heavy Oil and Oil sands Tech. Symposium, Calgary, 14 March

Mese A. I. and Tutuncu A. N., 2000. A Novel Experimental Technique for Investigation of Pore Pressure Effect on Acoustic and Mechanical Properties in Unconsolidated Shaly Sands and Shales, Pacific Rocks: Rock Around the Rim, 173- 179, Editors Girard, Liebman, Breeds and Doe, Balkema.

Metwally, M. & Solanki, S. (1995, January 1). Heavy Oil Reservoir Mechanisms, Linbergh and Frog Lake Fields, Alberta Part II: Geomechanical Evaluation. Society of Petroleum Engineers. doi:10.2118/30249-MS.

Mohamed, I. M., He, J., & Nasr-El-Din, H. A. (2011, January 1). Permeability Change during CO2 injection in Carbonate Rock: A Coreflood Study. Society of Petroleum Engineers. doi:10.2118/140943-MS

Morye, G.G., 2007. Equation of state model development and compositional simulation of enhanced oil recovery using gas injection for the West Sak heavy oil. University of Alaska Fairbanks, MS Thesis.

Muecke, T. W. (1979, February 1). Formation Fines and Factors Controlling Their Movement in Porous Media. Society of Petroleum Engineers. doi:10.2118/7007-PA

Muralidharan V., Erwin Putra, and David S. Schechter. 2005: Investigating the Changes in Matrix and Fracture Properties and Fluid Flow under Different Stress- state Conditions, Saudi Aramco. Journal of Technology.

Nourpour Aghbash. V, 2013. Evaluation of CO_2 sequestration through enhanced oil recovery in West Sak reservoir, University of Alaska Fairbanks, MS Thesis.

Ott W. K., Woods J. D, *Modern Sandface Completion Practices Handbook*, First edition, World Oil, Texas, 2001.

Panda, M. N., Zhang, M., Ogbe, D. O., Kamath, V. A., & Sharma, G. D. (1989, January 1). Reservoir Description of West Sak Sands Using Well Logs. Society of Petroleum Engineers. doi:10.2118/18759-MS

Patel, P. D., Christman, P. G., & Gardner, J. W. (1987, November 1). Investigation of Unexpectedly Low Field-Observed Fluid Mobilities During Some CO2 Tertiary Floods. Society of Petroleum Engineers. doi:10.2118/14308-PA

Penberthy, W.L. and Shaughnessy, C.M., Sand Control, SPE Series on. Special Topics, Volume 1, 1992.

Peng, D. Y., and Robinson, D. B. (1976). "A New Two-Constant Equation of State". Industrial and Engineering Chemistry: Fundamentals **15**: 59–64. doi:10.1021/i160057a011

Rui W., Xiang'an Y., Renbao Z., Pingxiang Y et al. 2009. Effect of stress sensitivity on displacement efficiency in CO_2 flooding for fractured low permeability reservoirs. Pet. Sci. Volume 6, Number 3 (2009), 277-283, DOI:10.1007/s12182-009-0044-6

Sanyal, S. K., Marsden, S. S., & Ramey, H. J. (1974, January 1). Effect of Temperature on Petrophysical Properties of Reservoir Rocks. Society of Petroleum Engineers. doi:10.2118/4898-MS

Saucier, R. J. (1974, February 1). Considerations in Gravel Pack Design. Society of Petroleum Engineers. doi:10.2118/4030-PA

Sharma, G., 1990. Development of Effective Gas Solvents Including Carbon Dioxide for the Improved Recovery of West Sak Oil, University of Alaska Fairbanks, AK.

Targac, G. W., Redman, R. S., Davis, E. R., Rennie, S. B., McKeever, S. O., & Chambers, B. C. (2005, January 1). Unlocking the Value in West Sak Heavy Oil. Society of Petroleum Engineers. doi:10.2118/97856-MS

Teklu, T. W., Alameri, W., Graves, R. M., Tutuncu, A. N., Kazemi, H., & Alsumaiti, A. M. (2012, October 30). Geomechanics Considerations in Enhanced Oil Recovery. Society of Petroleum Engineers. doi:10.2118/162701-MS

Terzaghi, Karl, Theoretical Soil Mechanics, *1943* John Wiley & Sons, NY.

Tiffin, D. L., King, G. E., Larese, R. E., & Britt, L. K. (1998, January 1). New Criteria for Gravel and Screen Selection for Sand Control. Society of Petroleum Engineers. doi:10.2118/39437-MS

Tiffin, D. L., Stein, M. H., & Wang, X. (2003, January 1). Drawdown Guidelines for Sand Control Completions. Society of Petroleum Engineers. doi:10.2118/84495-MS

Wedman, M. L., Lynch, K. W., & Spearman, J. W. (1999, January 1). Hydraulic Fracturing for Sand Control in Unconsolidated Heavy-Oil Reservoirs. Society of Petroleum Engineers. doi:10.2118/54628-MS

Werner, M., 1987. Tertiary and Upper Cretaceous Heavy Oil Sands, Kuparuk River Unit Area, Alaskan North Slope. Exploration for Heavy Crude Oil and Natural Bitumen: American Association of Petroleum Geologists Studies in Geology (25): 537 - 548.

Young, J. P., Mathews, W. L., & Hulm, E. (2010, January 1). Alaskan Heavy Oil: First CHOPS at a vast, untapped arctic resource. Society of Petroleum Engineers. doi:10.2118/133592-MS

Zekri, A. Y., & Chaalal, O. (2001, January 1). Thermal Stress of Carbonate Rocks: An Experimental Approach. Society of Petroleum Engineers. doi:10.2118/68777-MS

Zhou, J., Dong, Y., Pater, C. J., & Zitha, P. L. J. (2010, January 1). Experimental Study of the Impact of Shear Dilation and Fracture Behavior During Polymer Injection for Heavy Oil Recovery in Unconsolidated Reservoirs. Society of Petroleum Engineers. doi:10.2118/137656-MS

Appendix

1. Input file for case with geomechanics at varying injector CBHP

```
** 2014-08-02, 4:33:20 AM, Nitesh Chauhan
RESULTS SIMULATOR STARS 201210
INUNIT FIELD
TITLE2 'waterfood sand'
WSRF WELL 1
WSRF GRID 5
WSRF SECTOR 5
WSRF GRIDDEFORM 5
OUTSRF GRID BIOT BULKVOL FPOROS GCOHESION GEORTYPE PERMI PERMJ
PERMK POISSON PORDIFF PRES
        OUTSRF WELL DOWNHOLE
OUTSRF WELL COMPONENT ALL
WPRN GRID 0
OUTPRN GRID ALL
OUTPRN RES ALL
OUTPRN WELL ALL
**$  Distance units: ft
RESULTS XOFFSET          0.0000
RESULTS YOFFSET          0.0000
RESULTS ROTATION          0.0000  **$  (DEGREES)
RESULTS AXES-DIRECTIONS 1.0 -1.0 1.0
**$
***************************************************************************
**$ Definition of fundamental cartesian grid
**$
***************************************************************************
GRID VARI 25 25 9
KDIR DOWN
```

```
DI IVAR
 25*52.8
DJ JVAR
 25*52.8
DK ALL
 625*40 625*30 625*26 625*20 625*26 625*9 625*65 625*16 625*38
DTOP
 625*3544
PVCUTOFF 0
NETPAY KVAR
 30 0 21 0 3 0 3 0 17
**$  0 = null block, 1 = active block
NULL CON            1
POR KVAR
 0.3 0 0.31 0 0.23 0 0.25 0 0.27
PERMI KVAR
 150 0 150 0 150 0 150 0 150
PERMJ KVAR
 150 0 150 0 150 0 150 0 150
PERMK CON            0
**$  0 = pinched block, 1 = active block
PINCHOUTARRAY CON            1
END-GRID
ROCKTYPE 1
PRPOR 1700
CPOR 0.000005
PORINTERP REF
THCONR 24
THCONW 24
THCONO 24
THCONG 24
```

```
********************************************************************************
**
** THE FOLLOWING KEYWORDS CAN BE USED IN THE INITIALIZATION SECTION IN STARS
********************************************************************************
**
** MFRAC_OIL 'CO2     ' CON  1.5810E-04
** MFRAC_OIL 'N2      ' CON  2.8421E-04
** MFRAC_OIL 'CH4     ' CON  3.6675E-01
** MFRAC_OIL 'C2H6    ' CON  8.5689E-03
** MFRAC_OIL 'C3H8    ' CON  3.6340E-03
** MFRAC_OIL 'NC4     ' CON  1.8218E-03
** MFRAC_OIL 'NC5     ' CON  6.5291E-04
** MFRAC_OIL 'FC6     ' CON  2.0423E-03
** MFRAC_OIL 'C7 toHYP' CON  6.1609E-01
********************************************************************************
**
** THE FOLLOWING SECTION CAN BE USED FOR THE COMPONENT PROPERTY INPUT INTO STARS
********************************************************************************
**
** PVT UNITS CONSISTENT WITH *INUNIT *FIELD
**$ Model and number of components
**$ Model and number of components
**$ Model and number of components
**$ Model and number of components
**$ Model and number of components
**$ Model and number of components
**$ Model and number of components
**$ Model and number of components
MODEL 10 10 10 1
```

```
COMPNAME 'WATER' 'CO2' 'N2' 'CH4' 'C2H6' 'C3H8' 'NC4' 'NC5' 'FC6' 'C7 toHYP'
**        --------  --------  --------  --------  --------  --------  --------  --------  --------  --------
CMM
0 44.01 28.013 16.043 30.07 44.097 58.124 72.151 86 369.062
PCRIT
0 1069.87 492.31 667.2 708.34 615.76 551.1 489.38 477.03 183.5
TCRIT
0.00 87.89 -232.51 -116.59 90.05 205.97 305.69 385.61 453.83 1353.61
** reference pressure,     corresponding to the density
PRSR 1600
** reference temperature,  corresponding to the density
TEMR 80
** pressure at surface,    for reporting well rates, etc.
PSURF 14.696
** temperature at surface, for reporting well rates, etc.
TSURF 60
**$ Surface conditions
SURFLASH KVALUE
K_SURF 'CO2' 70.439
K_SURF 'N2' 569.49
K_SURF 'CH4' 184.75
K_SURF 'C2H6' 32.367
K_SURF 'C3H8' 8.5206
K_SURF 'NC4' 2.2845
K_SURF 'NC5' 0.62257
K_SURF 'FC6' 0.21975
K_SURF 'C7 toHYP' 1.4288e-011
MOLDEN
0 1.296 1.311 1.254 1.008 0.8048 0.6688 0.5634 0.5191 0.1601
CP
```

0 3.039e-005 3.757e-005 3.455e-005 2.359e-005 1.835e-005 1.485e-005 1.227e-005 1.095e-005 3.268e-006

CT1

0 0.000966 0.001114 0.0009588 0.0005927 0.0003721 0.0002544 0.0001789 0.0001493 0.0002524

CT2

0 6.94e-007 7.74e-007 8.701e-007 8.18e-007 8.208e-007 7.669e-007 7.037e-007 6.615e-007 1.17e-007

CPT

0 1.183e-005 9.24e-006 2.443e-007 -2.951e-008 -2.369e-008 2.81e-008 6.838e-006 -1.839e-007 5.848e-010

** T, deg F 'WATER' 'CO2' 'N2' 'CH4' 'C2H6' 'C3H8' 'NC4' 'NC5' 'FC6' 'C7 toHYP'

** -------- -------- -------- -------- -------- -------- -------- -------- -------- --------

**$ temp

VISCTABLE

*ATPRES 100

**$ temp

10 0 19.434 7.9599 7.9391 12.448 15.112 17.945 20.737 23.823 165.32

36.667 0 18.748 7.8756 7.8127 12.072 14.516 17.087 19.565 22.33 137.88

63.333 0 17.917 7.6996 7.6011 11.593 13.82 16.14 18.329 20.797 115.62

90 0 16.967 7.4428 7.3155 11.026 13.042 15.124 17.049 19.241 97.305

116.667 0 15.93 7.1192 6.9696 10.393 12.206 14.064 15.747 17.686 82.077

143.333 0 14.835 6.7435 6.578 9.7138 11.335 12.983 14.448 16.156 69.327

170 0 13.711 6.3303 6.1545 9.0076 10.449 11.904 13.173 14.672
58.599

196.667 0 12.584 5.8934 5.7123 8.292 9.5665 10.845 11.94 13.249
49.541

223.333 0 11.474 5.4446 5.2625 7.5815 8.703 9.8217 10.761 11.901
41.878

250 0 10.397 4.9944 4.8148 6.8881 7.8706 8.8449 9.6486 10.636
35.384

*ATPRES 977.778

**$ temp

10 0 31.722 12.993 12.959 20.318 24.668 29.291 33.848 38.886
269.85

36.667 0 28.924 12.151 12.054 18.626 22.396 26.362 30.186 34.452
212.72

63.333 0 26.32 11.311 11.166 17.03 20.301 23.709 26.926 30.551
169.85

90 0 23.897 10.483 10.303 15.53 18.369 21.301 24.012 27.099
137.05

116.667 0 21.641 9.6715 9.4684 14.119 16.582 19.106 21.393 24.027
111.5

143.333 0 19.54 8.882 8.664 12.794 14.929 17.101 19.03 21.28
91.312

170 0 17.585 8.1189 7.8934 11.553 13.401 15.268 16.895 18.817
75.155

196.667 0 15.772 7.3867 7.1597 10.393 11.99 13.593 14.965 16.606
62.094

223.333 0 14.097 6.6895 6.4657 9.3149 10.693 12.067 13.222 14.622
51.453

250 0 12.555 6.0308 5.8139 8.3175 9.5037 10.68 11.651 12.843
42.727

*ATPRES 1855.56

**$ temp
10 0 33.998 13.925 13.888 21.776 26.437 31.392 36.276 41.675
289.2
36.667 0 31.092 13.061 12.957 20.022 24.075 28.338 32.448 37.034
228.66
63.333 0 28.156 12.1 11.945 18.218 21.718 25.364 28.805 32.682
181.7
90 0 25.279 11.089 10.899 16.428 19.431 22.532 25.4 28.666
144.97
116.667 0 22.524 10.066 9.8549 14.696 17.259 19.886 22.266 25.008
116.06
143.333 0 20.171 9.1691 8.944 13.208 15.412 17.653 19.645 21.968
94.264
170 0 18.119 8.3655 8.1332 11.904 13.808 15.731 17.408 19.388
77.437
196.667 0 16.206 7.5896 7.3564 10.679 12.32 13.967 15.376 17.062
63.801
223.333 0 14.436 6.8502 6.6211 9.5388 10.95 12.357 13.54 14.973
52.689
250 0 12.81 6.1531 5.9318 8.4862 9.6965 10.897 11.887 13.104
43.593
*ATPRES 2733.33
**$ temp
10 0 36.021 14.754 14.715 23.072 28.011 33.261 38.435 44.155
306.41
36.667 0 33.141 13.922 13.811 21.341 25.661 30.206 34.587 39.474
243.73
63.333 0 30.204 12.98 12.814 19.543 23.297 27.208 30.899 35.059
194.91
90 0 27.301 11.976 11.771 17.742 20.985 24.335 27.432 30.959
156.57

116.667 0 24.501 10.95 10.72 15.985 18.774 21.63 24.22 27.203
126.24
143.333 0 21.85 9.9322 9.6884 14.307 16.694 19.122 21.28 23.796
102.11
170 0 19.378 8.9466 8.6981 12.73 14.767 16.824 18.618 20.735
82.817
196.667 0 17.102 8.0093 7.7632 11.269 13.001 14.739 16.227 18.005
67.329
223.333 0 15.028 7.1313 6.8927 9.9301 11.399 12.864 14.095 15.587
54.851
250 0 13.155 6.3189 6.0917 8.7148 9.9578 11.191 12.207 13.457
44.768
*ATPRES 3611.11
**$ temp
10 0 37.953 15.545 15.504 24.309 29.513 35.045 40.497 46.523
322.85
36.667 0 35.102 14.746 14.628 22.604 27.179 31.992 36.633 41.809
258.15
63.333 0 32.167 13.824 13.647 20.814 24.812 28.977 32.908 37.338
207.58
90 0 29.246 12.829 12.609 19.006 22.48 26.068 29.386 33.165
167.72
116.667 0 26.407 11.802 11.554 17.229 20.234 23.313 26.104 29.319
136.06
143.333 0 23.702 10.774 10.51 15.52 18.109 20.743 23.084 25.813
110.76
170 0 21.163 9.7705 9.4991 13.903 16.127 18.373 20.332 22.645
90.443
196.667 0 18.809 8.8088 8.5381 12.394 14.299 16.21 17.846 19.803
74.049

223.333 0 16.65 7.901 7.6368 11.002 12.63 14.253 15.617 17.27
60.771

250 0 14.687 7.0549 6.8012 9.7299 11.118 12.494 13.629 15.024
49.983

*ATPRES 4488.89

**$ temp

10 0 39.798 16.301 16.258 25.491 30.948 36.749 42.466 48.786
338.55

36.667 0 36.978 15.534 15.41 23.812 28.632 33.703 38.591 44.045
271.95

63.333 0 34.051 14.633 14.446 22.033 26.265 30.674 34.835 39.525
219.74

90 0 31.115 13.649 13.416 20.221 23.917 27.735 31.265 35.285
178.44

116.667 0 28.245 12.623 12.358 18.428 21.643 24.936 27.921 31.36
145.53

143.333 0 25.492 11.588 11.303 16.692 19.477 22.31 24.828 27.763
119.13

170 0 22.893 10.569 10.276 15.04 17.446 19.876 21.995 24.496
97.839

196.667 0 20.47 9.5866 9.292 13.488 15.562 17.642 19.422 21.551
80.588

223.333 0 18.234 8.6526 8.3632 12.048 13.831 15.609 17.102 18.912
66.552

250 0 16.189 7.7762 7.4966 10.725 12.254 13.771 15.023 16.561
55.093

*ATPRES 5366.67

**$ temp

10 0 41.563 17.023 16.979 26.621 32.32 38.378 44.348 50.948
353.55

36.667 0 38.776 16.289 16.159 24.969 30.024 35.341 40.467 46.185
285.17
63.333 0 35.859 15.41 15.213 23.203 27.659 32.302 36.685 41.623
231.41
90 0 32.914 14.438 14.191 21.39 25.299 29.338 33.071 37.324
188.76
116.667 0 30.016 13.415 13.133 19.584 23 26.5 29.672 33.326
154.66
143.333 0 27.222 12.374 12.071 17.825 20.799 23.824 26.513 29.647
127.21
170 0 24.57 11.343 11.028 16.141 18.723 21.331 23.606 26.29
105
196.667 0 22.083 10.342 10.024 14.552 16.788 19.032 20.953 23.25
86.94
223.333 0 19.777 9.385 9.071 13.068 15.002 16.93 18.55 20.513
72.185
250 0 17.657 8.4813 8.1763 11.697 13.365 15.02 16.385 18.062
60.088
*ATPRES 6244.44
**$ temp
10 0 43.251 17.715 17.668 27.702 33.632 39.936 46.149 53.017
367.91
36.667 0 40.498 17.012 16.877 26.078 31.357 36.91 42.264 48.236
297.83
63.333 0 37.594 16.156 15.949 24.325 28.998 33.865 38.46 43.637
242.6
90 0 34.643 15.196 14.937 22.513 26.629 30.879 34.809 39.285
198.67
116.667 0 31.723 14.177 13.88 20.698 24.308 28.007 31.359 35.222
163.45

143.333 0 28.893 13.134 12.811 18.919 22.076 25.286 28.14 31.467
135.02

170 0 26.193 12.093 11.757 17.207 19.96 22.741 25.165 28.027
111.94

196.667 0 23.649 11.076 10.735 15.583 17.979 20.382 22.439 24.899
93.105

223.333 0 21.279 10.098 9.7599 14.061 16.141 18.215 19.958 22.071
77.667

250 0 19.089 9.1694 8.8397 12.646 14.45 16.239 17.714 19.528
64.963

*ATPRES 7122.22

**$ temp

10 0 44.867 18.376 18.329 28.737 34.889 41.428 47.874 54.998
381.66

36.667 0 42.149 17.706 17.565 27.142 32.636 38.415 43.987 50.203
309.98

63.333 0 39.261 16.872 16.656 25.404 30.283 35.367 40.165 45.571
253.36

90 0 36.307 15.926 15.654 23.595 27.908 32.362 36.481 41.172
208.21

116.667 0 33.369 14.913 14.6 21.771 25.569 29.459 32.986 37.048
171.93

143.333 0 30.506 13.867 13.527 19.975 23.309 26.698 29.711 33.224
142.56

170 0 27.763 12.818 12.462 18.239 21.157 24.104 26.674 29.708
118.65

196.667 0 25.168 11.787 11.425 16.584 19.133 21.691 23.88 26.498
99.084

223.333 0 22.739 10.79 10.429 15.025 17.248 19.465 21.328 23.585
82.995

```
      250        0   20.485    9.8399    9.4861    13.571    15.506    17.426     19.01    20.956
69.714
 *ATPRES 8000
**$    temp
       10        0   46.415    19.011    18.961    29.729    36.093    42.858    49.526    56.896
394.83
   36.667        0   43.733    18.372    18.225    28.162    33.863    39.859    45.641     52.09
321.63
   63.333        0   40.862     17.56    17.335    26.439    31.518    36.809    41.803     47.43
263.69
       90        0   37.908    16.628    16.344    24.635    29.138    33.789    38.089    42.987
217.39
  116.667        0   34.954    15.621    15.293    22.805    26.784    30.859    34.553    38.809
180.1
  143.333        0   32.064    14.575    14.218    20.995    24.499    28.062    31.228     34.92
149.84
      170        0   29.283    13.519    13.144    19.237    22.315    25.423    28.133    31.333
125.15
  196.667        0    26.64    12.476    12.093    17.554    20.252     22.96    25.276    28.047
104.88
  223.333        0   24.157    11.463     11.08    15.962    18.324    20.679    22.657    25.056
88.171
      250        0   21.844    10.493    10.115    14.471    16.535    18.582    20.271    22.346
74.338

** The following is the complete WinProp fluid model description.

WINPROP *TITLE1    ''
WINPROP *TITLE2    ''
WINPROP *TITLE3    ''
WINPROP *INUNIT *FIELD
```

```
WINPROP *MODEL   *PR   *1978
WINPROP *NC       9     9
WINPROP *TRANSLATION 3
WINPROP *PVC3  6.3167328E-01
WINPROP *COMPNAME
WINPROP 'CO2     ' 'N2      ' 'CH4     ' 'C2H6    ' 'C3H8    '
WINPROP 'NC4     ' 'NC5     ' 'FC6     ' 'C7 toHYP'
WINPROP *HCFLAG
WINPROP   3  0  1  1  1  1  1  1  1
WINPROP *SG
WINPROP   8.1800000E-01  8.0900000E-01  3.0000000E-01  3.5600000E-01  5.0700000E-01
WINPROP   5.8400000E-01  6.3100000E-01  6.9000000E-01  8.6735991E-01
WINPROP *TB
WINPROP   -1.0921000E+02  -3.2035000E+02  -2.5861000E+02  -1.2757000E+02  -
4.3690000E+01
WINPROP   3.1190000E+01  9.6890000E+01  1.4693000E+02  7.9825434E+02
WINPROP *PCRIT
WINPROP   7.2800000E+01  3.3500000E+01  4.5400000E+01  4.8200000E+01
4.1900000E+01
WINPROP   3.7500000E+01  3.3300000E+01  3.2460000E+01  1.2486281E+01
WINPROP *VCRIT
WINPROP   9.4000000E-02  8.9500000E-02  9.9000000E-02  1.4800000E-01  2.0300000E-01
WINPROP   2.5500000E-01  3.0400000E-01  3.4400000E-01  1.3196352E+00
WINPROP *TCRIT
WINPROP   3.0420000E+02  1.2620000E+02  1.9060000E+02  3.0540000E+02
3.6980000E+02
WINPROP   4.2520000E+02  4.6960000E+02  5.0750000E+02  1.0073800E+03
WINPROP *AC
WINPROP   2.2500000E-01  4.0000000E-02  8.0000000E-03  9.8000000E-02  1.5200000E-01
WINPROP   1.9300000E-01  2.5100000E-01  2.7504000E-01  6.3469000E-01
WINPROP *MW
```

WINPROP 4.4010000E+01 2.8013000E+01 1.6043000E+01 3.0070000E+01 4.4097000E+01

WINPROP 5.8124000E+01 7.2151000E+01 8.6000000E+01 3.6906190E+02

WINPROP *BIN

WINPROP 0.0000000E+00

WINPROP 1.0500000E-01 2.5000000E-02

WINPROP 1.3000000E-01 1.0000000E-02

WINPROP 1.2500000E-01 9.0000000E-02

WINPROP 1.1500000E-01 9.5000000E-02

WINPROP 1.1500000E-01 1.1000000E-01

WINPROP 1.1500000E-01 1.1000000E-01

WINPROP 1.3773960E-01 1.1649703E-01

WINPROP *VSHIFT

WINPROP 0.0000000E+00 0.0000000E+00 0.0000000E+00 0.0000000E+00 0.0000000E+00

WINPROP 0.0000000E+00 0.0000000E+00 0.0000000E+00 2.8579459E-01

WINPROP *VSHIF1

WINPROP 0.0000000E+00 0.0000000E+00 0.0000000E+00 0.0000000E+00 0.0000000E+00

WINPROP 0.0000000E+00 0.0000000E+00 0.0000000E+00 -1.2704957E-04

WINPROP *TREFVS

WINPROP 6.0000000E+01 6.0000000E+01 6.0000000E+01 6.0000000E+01 6.0000000E+01

WINPROP 6.0000000E+01 6.0000000E+01 6.0000000E+01 6.0000000E+01

WINPROP *ZRA

WINPROP 2.7360000E-01 2.9050000E-01 2.8760000E-01 2.7890000E-01 2.7630000E-01

WINPROP 2.7280000E-01 2.6850000E-01 2.7126127E-01 2.3740672E-01

WINPROP *VISVC

WINPROP 9.4000000E-02 8.9500000E-02 6.3360000E-02 1.4800000E-01 2.0300000E-01

WINPROP 2.5500000E-01 3.0400000E-01 3.4400000E-01 1.7074661E+00

WINPROP *MIXVC 1.0000000E+00

WINPROP *VISCOEFF

WINPROP 1.0230000E-01 2.3364000E-02 5.8533000E-02 -4.0758000E-02 9.3324000E-03

WINPROP *OMEGA

WINPROP 4.5723553E-01 4.5723553E-01 4.5723553E-01 4.5723553E-01 4.5723553E-01

WINPROP 4.5723553E-01 4.5723553E-01 4.5723553E-01 4.5723553E-01

WINPROP *OMEGB

WINPROP 7.7796074E-02 7.7796074E-02 7.7796074E-02 7.7796074E-02 7.7796074E-02

WINPROP 7.7796074E-02 7.7796074E-02 7.7796074E-02 7.7796074E-02

WINPROP *PCHOR

WINPROP 7.8000000E+01 4.1000000E+01 7.7000000E+01 1.0800000E+02 1.5030000E+02

WINPROP 1.8990000E+02 2.3150000E+02 2.5010880E+02 7.9628407E+02

WINPROP *HREFCOR *HARVEY

WINPROP *IGHCOEF

WINPROP 9.6880000E-02 1.5884300E-01 -3.3712000E-05 1.4810500E-07 -9.6620300E-11 2.0738320E-14 1.5114700E-01

WINPROP -6.5665000E-01 2.5409800E-01 -1.6624000E-05 1.5302000E-08 -3.0995000E-12 1.5167000E-16 4.8679000E-02

WINPROP -2.8385700E+00 5.3828500E-01 -2.1140900E-04 3.3927600E-07 -1.1643220E-10 1.3896120E-14 -6.0286900E-01

WINPROP -1.4220000E-02 2.6461200E-01 -2.4568000E-05 2.9140200E-07 -1.2810330E-10 1.8134820E-14 8.3346000E-02

WINPROP 6.8715000E-01 1.6030400E-01 1.2608400E-04 1.8143000E-07 -9.1891300E-11 1.3548500E-14 2.6090300E-01

WINPROP 7.2281400E+00 9.9687000E-02 2.6654800E-04 5.4073000E-08 -4.2926900E-11 6.6958000E-15 3.4597400E-01

WINPROP 9.0420900E+00 1.1182900E-01 2.2851500E-04 8.6331000E-08 -5.4464900E-11 8.1845000E-15 1.8318900E-01

WINPROP 0.0000000E+00 -1.6543463E-02 4.1169069E-04 -5.7742757E-08 0.0000000E+00 0.0000000E+00 0.0000000E+00

```
WINPROP   0.0000000E+00 -2.6430504E-03  4.0200655E-04 -5.4927343E-08  0.0000000E+00
0.0000000E+00  0.0000000E+00
WINPROP *HEATING_VALUES
WINPROP        0.0000000E+00      0.0000000E+00      8.4429001E+02      1.4784600E+03
2.1051600E+03
WINPROP   2.7115400E+03  3.3536600E+03  3.9759100E+03  3.4242512E+03
WINPROP *COMPOSITION *PRIMARY
WINPROP   1.5950289E-04  3.1900577E-04  3.8213901E-01  8.5433733E-03  3.5788460E-03
WINPROP   1.7844385E-03  6.3801154E-04  1.9937861E-03  6.0084403E-01
ROCKFLUID
RPT 1 WATWET
**$      Sw       krw       krow
**      Sw       krw       krow
**$       Sw       krw       krow
SWT
    0.45762748          0          1
    0.51285666  0.009306123    0.8373114
     0.5645018  0.015814025   0.49284938
      0.619148   0.06934746   0.22395943
     0.6613333  0.101493955   0.10037533
     0.7143854   0.14851725  0.017977355
     0.7484025   0.18102205  0.003299861
     0.7602694   0.19366163  0.001710956
             1            1            0
**$      Sl       krg       krog
**      Sl       krg       krog
**$       Sl       krg       krog
SLT
    0.45762748          1     0.00E+00
    0.53028697   0.8568176     5.99E-04
     0.6107928   0.55631757  0.001599789
```

```
  0.6907153   0.3341441  0.002601287
  0.7432232  0.21929157  0.018648729
 0.83834803  0.08079533   0.15053768
  0.9271493 0.015267108    0.6365089
  0.9803129 0.002346739    0.9261604
          1           0            1
RPT 2 WATWET
**$       Sw        krw        krow
**      Sw        krw        krow
**$        Sw        krw        krow
SWT
 0.33236495           0            1
 0.33745348 0.001776372    0.9438472
 0.38166472 0.007186858    0.6112493
  0.4389437 0.009104184   0.30517668
 0.49810582 0.014558691  0.113853425
  0.5430241 0.015560039   0.04251845
  0.5768076 0.018298632  0.016158631
  0.6135985 0.018394675  0.003048974
  0.6377818     0.01934  0.001369082
          1           1            0
**$       Sl      krg        krog
**      Sl      krg        krog
**$        Sl        krg        krog
SLT
 0.33236495           1            0
 0.36101317   0.9609065        0.004
 0.47587988   0.7956798  0.005258618
  0.5787399   0.6450982  0.005301314
  0.6575837  0.52514535  0.005398723
  0.7048844  0.45585096  0.005709339
```

```
   0.7762237   0.34521857  0.022592802
   0.8377878    0.2559395   0.09662962
   0.8775895    0.1932883    0.1932883
  0.91362923   0.13998258    0.3314152
   0.9316547  0.110652424    0.4413101
   0.9624437   0.06266627   0.66241354
  0.98046637   0.03467476    0.8191714
  0.98948747  0.015993716   0.92366666
  0.99624354  0.006668223    0.9772579
           1            0            1
RPT 3 WATWET
**$        Sw         krw        krow
**        Sw         krw        krow
**$          Sw          krw         krow
SWT
  0.35351747            0            1
   0.3716089        0.003    0.9464388
       0.378     0.006965   0.85933447
  0.40570185  0.021440033   0.59029424
  0.43821093  0.036923423     0.416827
  0.47073638   0.05433488    0.2770564
    0.506503   0.07840554   0.15360019
  0.52783555  0.090344414   0.09805668
   0.5582792    0.1126354  0.031626865
    0.581808   0.13319121  0.005894218
   0.5924865    0.1406067  0.002735012
   0.5999729    0.1471472  0.001533551
           1            1            0
**$        Sl        krg         krog
**        Sl        krg         krog
**$          Sl          krg         krog
```

```
SLT
 0.35351747          1          0
  0.3880279   0.9217364    5.81E-04
 0.45319542  0.79720294  0.002181106
  0.5080974   0.6896653   0.00262148
 0.56302595  0.59113634  0.003326323
  0.6058951  0.51863027  0.004003477
  0.6596465   0.4325005  0.004588385
  0.7164152   0.3407096  0.005142544
  0.7581006  0.27835062  0.005230512
 0.79132104  0.22621249  0.005518361
 0.86144215  0.13541235   0.04646397
  0.9043743  0.08430192   0.14850104
  0.9340103 0.051344126   0.27994543
  0.9618459 0.025161294   0.47785345
  0.9812197 0.010325403   0.73101336
 0.99212515 0.004584285    0.9358562
          1           0           1
RTYPE KVAR
 2*1 2 3*1 2 1 3
INITIAL
VERTICAL DEPTH_AVE

INITREGION 1
REFPRES 1603.8
REFDEPTH 3544
DWOC 3800
SW KVAR
 0.24 0 0.31 0 0.45 0 0.47 0 0.41
MFRAC_OIL 'NC5' CON  0.000638012
MFRAC_OIL 'NC4' CON   0.00178444
```

```
MFRAC_OIL 'N2' CON  0.000319006
MFRAC_OIL 'FC6' CON   0.00199379
MFRAC_OIL 'CO2' CON  0.000159503
MFRAC_OIL 'CH4' CON     0.382139
MFRAC_OIL 'C7 toHYP' CON     0.600844
MFRAC_OIL 'C3H8' CON   0.00357885
MFRAC_OIL 'C2H6' CON   0.00854337

** ============= GEOMECHANIC MODEL ====================
GEOMECH
GEOM3D

NITERGEO 500

GEOROCK 1
POISSRATIO 0.37
ELASTMOD 100000
COHESION 100

STRESS3D  2500  2500  2500  0.0  0.0  0.0

GCOUPLING 2
**NODE8
```

2. Input file for case with geomechanics at varying injection rate

Same code is used except the input parameters for well are substituted with the following code:

```
WELL  'Well-1'
INJECTOR UNWEIGHT 'Well-1'
INCOMP  WATER  1.0  0.0  0.0  0.0  0.0  0.0  0.0  0.0  0.0  0.0
PINJW  1600.0
OPERATE  MAX  STW  1000.0  CONT
```